PTEP

Prog. Theor. Exp. Phys. **2023** (27 pages)
DOI: 10.1093/ptep/ptad092

$(g-2)_{e,\mu}$ and decays $e_b \to e_a \gamma$ in a $SU(4)_L \otimes U(1)_X$ model with inverse seesaw neutrinos

N. H. Thao[1], D. T. Binh[2,3], T. T. Hong[4], L. T. Hue[5,6], and D. P. Khoi[7,*]

[1]*Department of Physics, Hanoi Pedagogical University 2, no. 32 Nguyen Van Linh, Phuc Yen, Vinh Phuc 280000, Vietnam*
[2]*Institute of Theoretical and Applied Research, Duy Tan University, Hanoi, Vietnam*
[3]*Faculty of Natural Science, Duy Tan University, Da Nang, Vietnam*
[4]*Faculty of Engineering, Technology and Environment, An Giang University, VNU - HCM, Ung Van Khiem Street, Long Xuyen, An Giang 880000, Vietnam*
[5]*Subatomic Physics Research Group, Science and Technology Advanced Institute, Van Lang University, Ho Chi Minh City, Vietnam*
[6]*Faculty of Applied Technology, School of Technology, Van Lang University, Ho Chi Minh City, Vietnam*
[7]*Department of Physics, Vinh University, 182 Le Duan, Vinh City, Nghe An, Vietnam*
*E-mail: khoidp@vinhuni.edu.vn.

Received February 20, 2023; Revised June 8, 2023; Accepted July 2, 2023; Published July 6, 2023

We will show that the 3-4-1 model with heavy right-handed neutrinos can explain the recent experimental data of $(g-2)_{e,\mu}$ anomalies of charged leptons and neutrino oscillations through the inverse seesaw mechanism. In addition, the model can predict large lepton flavor violating decay rates $\mu \to e\gamma$ and $\tau \to \mu\gamma, e\gamma$ with accuracy equal to recent experimental sensitivities.

Subject Index B53, B56, B59

1. Introduction

The 3-4-1 model with right-handed neutrinos (341RHN) was discussed in Refs. [1,2] as a natural extension in which new right-handed neutrinos are assigned into the same left-handed lepton quadruplets. For a complete study of the highest possible gauge symmetry in the electroweak (EW) sector [3], various 3-4-1 extensions were introduced with different electric charges of new exotic leptons [4–12]. It was proved that these original 3-4-1 models cannot explain the recent data of the muon $(g-2)$ anomaly unless they are extended such as by adding new inert scalars [13]. A solution applied to the 3-3-1 models [14], that of adding new singly charged Higgs bosons and inverse seesaw (ISS) neutrinos, is another viable approach. In this work, we will investigate the possibility of whether this approach can work in the 3-4-1 model framework, which can accommodate data of charged lepton anomalies $a_{e_a} \equiv (g-2)_{e_a}/2$, neutrino oscillation data, and the recent bounds of the lepton flavor violating decays of charged leptons (cLFV) $e_b \to e_a\gamma$. The explanations of neutrino oscillation data were mentioned previously in various 3-4-1 models, including the ISS mechanism [10,15,16], but they did not relate to the $(g-2)$ data and cLFV decays. In the ISS models, new gauge contributions to $(g-2)$ are suppressed [16,17], especially the 3-3-1 and 3-4-1 models, because the new gauge bosons must be heavy to guarantee the recent lower bounds from experimental searches [18]. Therefore, we will

study the appearance of new singly charged Higgs bosons and their mixing with the $SU(4)_L$ ones that results in large chirally enhanced one-loop Higgs contributions to a_{e_a} enough to be consistent with experiments [19]. On the other hand, the ISS mechanism may lead to large one-loop contributions to cLFV rates. In this work, numerical investigations to determine the allowed regions of parameter space satisfying all experimental constraints of $(g-2)$ anomalies and cLFV decays $e_b \to e_a\gamma$ will be discussed precisely in the 3-4-1 framework. Besides many available models beyond the standard model (BSM) [20–42] under various experimental data including the $(g-2)_{e,\,\mu}$ anomalies, our work will confirm the reality of the 3-4-1 models.

The latest experimental measurement for the muon anomaly a_μ has been reported from the combination of the two experimental results at Fermilab [43] and Brookhaven National Laboratory (BNL) E82 [44]: $a_\mu^{\rm exp} = 116592061(41) \times 10^{-11}$. It leads to a standard deviation of 4.2 σ (standard deviation) from the Standard Model (SM) prediction, namely,

$$\Delta a_\mu^{\rm NP} \equiv a_\mu^{\rm exp} - a_\mu^{\rm SM} = (2.51 \pm 0.59) \times 10^{-9}, \tag{1}$$

where $a_\mu^{\rm SM} = 116591810(43) \times 10^{-11}$ is the SM prediction [45] combined from various different contributions based on the dispersion approach [46–72]. Another larger SM value calculated using the lattice-quantum chromodynamics (QCD) technique implies a smaller value of $\Delta a_\mu^{\rm NP}$ than that given in Eq. (1) [73]. In this work we will accept the experimental constraint from Eq. (1) consisting of both results. On the other hand, recent experimental a_e data were reported from different groups [74–76,77], leading to two inconsistent deviations between experiments and the SM prediction [78–83]. In this work, we accept the following value:[1]

$$\Delta a_e^{\rm NP} \equiv a_e^{\rm exp} - a_e^{\rm SM} = (3.4 \pm 1.6) \times 10^{-13}, \tag{2}$$

where we have used the latest experimental result of $a_e^{\rm exp}$ reported in Ref. [77], consistent with the 2008 result of the same group [74], and the $a_e^{\rm SM}$ value reported in Ref. [76], derived indirectly from the measurement of the fine-structure constant α using Rb atoms, corresponding to a 2.1σ deviation. There is another $a_e^{\rm SM}$ value corresponding to the measurement of the fine-structure constant of Cs-133 atoms [75], which is inconsistent with the earlier, namely $\Delta a_e^{\rm NP} = (-10.2 \pm 2.6) \times 10^{-13}$, with the 3.9σ deviation. Both results can be explained in this work, see details later in the numerical investigation.

The ISS mechanism may result in large values of not only $(g-2)_{e,\,\mu}$ but also ${\rm Br}(e_b \to e_a\gamma)$, which are constrained by recent experiments [84–86]:

$$\begin{aligned} {\rm Br}(\tau \to \mu\gamma) &< 4.4 \times 10^{-8}, \\ {\rm Br}(\tau \to e\gamma) &< 3.3 \times 10^{-8}, \\ {\rm Br}(\mu \to e\gamma) &< 4.2 \times 10^{-13}. \end{aligned} \tag{3}$$

The future sensitivities for these decays are ${\rm Br}(\mu \to e\gamma) < 6 \times 10^{-14}$ [87], ${\rm Br}(\tau \to e\gamma) < 9.0 \times 10^{-9}$, and ${\rm Br}(\tau \to \mu\gamma) < 6.9 \times 10^{-9}$ [88,89]. Hence the correlations between a_{e_a} and cLFV decays $e_b \to e_a\gamma$ may give new predictions on both of these kinds of processes, namely whether large a_{e_a} will exclude the stricter experimental constraints of cLFV decays in the near future.

Our paper is arranged as follows. Section 2 presents all ingredients of a 3-4-1 model to calculate the $(g-2)_{e_a}$ data and cLFV decays. Section 3 introduces the 341ISS model to accommodate the recent $(g-2)_{e_a}$ data. In this model, the Yukawa Lagrangian and Higgs potential must respect a new global $U(1)_{\mathcal{L}}$ symmetry in order to guarantee the appearance of the ISS

[1] We thank the referee for providing us with the experimental value of a_e in Ref. [77].

mechanism, the mixing between singly charged Higgs bosons, and the Yukawa couplings resulting in large chirally enhanced one-loop contributions to $(g-2)_{e_a}$ anomalies. Section 4 will present detailed numerical results to determine the allowed regions of the parameter space that explain both experimental results of two $(g-2)_{e,\mu}$ anomalies and cLFV decays. Section 5 summarizes important results.

2. The model with Dirac active neutrinos

2.1. *Yukawa couplings and masses for fermions*

In this work, we will study the 3-4-1 model with heavy right-handed neutrinos and new singly charged leptons assigned in the three left-handed quadruplets [5,10]. This model is constructed based on the gauge symmetry $SU(3)_c \times SU(4)_L \times U(1)_X$, implying 16 EW gauge bosons. In addition, there are four neutral gauge bosons corresponding to the four diagonal generators of the EW group. Normally, the EW group is assumed to break to the final electric group through the following pattern: $SU(4)_L \times U(1)_X \to SU(3)_L \times U(1)_{X'} \to SU(2) \times U(1)_Y \to U(1)_{em}$, i.e. the 3-4-1 model can be considered as the extended version of 3-3-1 models [90,91]. The electric operator is defined as follows:

$$Q = T_3 + \frac{1}{\sqrt{3}}T_8 - \frac{2}{\sqrt{6}}T_{15} + X\mathbb{I}, \tag{4}$$

where $T_{3,\,8,\,15}$ are the diagonal generators of the $SU(4)$ group and X is the $U(1)$ charge, see precise forms corresponding to the quadruplet in e.g. Ref. [92].

The lepton sector consists of three left-handed quadruplets and respective right-handed singlets, namely,

$$\begin{aligned} &L_a = (\nu'_a\,, e'_a\,, E'_a\,, N'_a)^T_L \sim \left(1, 4, -\frac{1}{2}\right)\,,\ a = 1, 2, 3, \\ &e'_{aR},\ E'_{aR} \sim (1, 1, -1), \qquad \nu'_{aR},\ N'_{aR} \sim (1, 1, 0). \end{aligned} \tag{5}$$

The Higgs multiplets and non-zero vacuum expectation values (VEVs) of neutral components needed for generating all fermion masses are:

$$\begin{aligned} \chi &= \left(\chi^0_1\,, \chi^-_2\,, \chi^-_3\,, \chi^0_4\right)^T \sim \left(1, 4, -\frac{1}{2}\right),\ \langle\chi\rangle = \left(0\,, 0\,, 0\,, \frac{V}{\sqrt{2}}\right)^T, \\ \phi &= \left(\phi^+_1\,, \phi^0_2\,, \phi^0_3\,, \phi^+_4\right)^T \sim \left(1, 4, \frac{1}{2}\right),\ \langle\phi\rangle = \left(0\,, 0\,, \frac{\omega}{\sqrt{2}}\,, 0\right)^T, \\ \rho &= \left(\rho^+_1\,, \rho^0_2\,, \rho^0_3\,, \rho^+_4\right)^T \sim \left(1, 4, \frac{1}{2}\right),\ \langle\rho\rangle = \left(0\,, \frac{v_1}{\sqrt{2}}\,, 0\,, 0\right)^T, \\ \eta &= \left(\eta^0_1\,, \eta^-_2\,, \eta^-_3\,, \eta^0_4\right)^T \sim \left(1, 4, -\frac{1}{2}\right),\ \langle\eta\rangle = \left(\frac{v_2}{\sqrt{2}}\,, 0\,, 0\,, 0\right)^T. \end{aligned} \tag{6}$$

The lepton masses are generated from the following Yukawa interactions:

$$-\mathcal{L}_y = Y^N_{ab}\overline{L_a}\chi N'_{bR} + Y^E_{ab}\overline{L_a}\phi E'_{bR} + Y^e_{ab}\overline{L_a}\rho e'_{bR} + Y^\nu_{ab}\overline{L_a}\eta\nu'_{bR} + \text{H.c.}. \tag{7}$$

The model consists of quark multiplets that must be arranged to cancel the gauge anomalies, see e.g. a discussion in Ref. [11]. It can be seen that the quark masses can be constructed to satisfy the recent experimental data.

Table 1. $\mathcal{L}$ charges for multiplets in the 341RH.

Multiplet	χ	ϕ	η	ρ	L_a	ν'_{aR}	e'_{aR}	E'_{aR}	N'_{aR}	$Q_{\alpha L}$	Q_{3L}	u'_{aR}	d'_{aR}	$D'_{\alpha R}$	$U'_{\alpha R}$	U'_{3R}	D'_{3R}
$\mathcal{L}$ charge	1	1	-1	-1	0	1	1	-1	-1	1	-1	0	0	2	2	-2	-2

Table 2. Nonzero lepton number L of all fields in the 341RH.

Fields	χ_1^0	χ_2^-	ϕ_1^+	ϕ_2^0	ρ_3^0	ρ_4^+	η_3^-	η_4^0	$E'_{aL,R}$	$N'_{aL,R}$	$U'_{\alpha L,R}$	$D'_{\alpha L,R}$	$U'_{3L,R}$	$D'_{3L,R}$
L	2	2	2	2	-2	-2	-2	-2	-1	-1	2	2	-2	-2

The zero VEVs of some neutral Higgs components can be explained by considering a global symmetry called the general lepton number $\mathcal{L}$ defined as follows:

$$L = \frac{4}{\sqrt{3}}\left(T_8 + \frac{1}{\sqrt{2}}T_{15}\right) + \mathcal{L}\,, \tag{8}$$

where L is the normal lepton number. This formula is an extension of that introduced for a 3-3-1 model [93]. As a consequence, all singlets have $L(\text{singlet}) = \mathcal{L}(\text{singlet})$, namely $\mathcal{L}(u_{aR}) = \mathcal{L}(d_{aR}) = 0$, $\mathcal{L}(e_{aR}) = \mathcal{L}(\nu'_{aR}) = 1 = -\mathcal{L}(E_{aR}) = -\mathcal{L}(N'_{aR})$. The normal lepton L for a quadruplet is computed as follows:

$$L = \text{diag}\,(1+\mathcal{L}\,, 1+\mathcal{L}\,, -1+\mathcal{L}\,, -1+\mathcal{L})\,. \tag{9}$$

In this work, we adopt only the Yukawa couplings respecting the generalized lepton number $\mathcal{L}$ including the Lagrangian (7) for leptons. The particular values of $\mathcal{L}$ of all multiplets are listed in Table 1.

They result in consistent values of the normal lepton numbers for all SM leptons $L(\nu'_{aL,R}) = L(e'_{aL,R}) = 1$, and all SM quarks have $L = 0$. The remaining non-zero lepton numbers L are listed in Table 2, because of the requirement that the total lepton number L is always conservative.

The mass terms of all leptons are:

$$(M_\nu)_{ab} = Y^\nu_{ab}\frac{v_2}{\sqrt{2}}\,,\ (M_e)_{ab} = Y^e_{ab}\frac{v_1}{\sqrt{2}}\,,\ (M_E)_{ab} = Y^E_{ab}\frac{\omega}{\sqrt{2}},\ (M_N)_{ab} = Y^N_{ab}\frac{V}{\sqrt{2}}. \tag{10}$$

The active Dirac neutrino masses and mixing are constructed from the mass matrix M_ν. But, these tiny masses do not affect significantly the one-loop contributions to a_{e_a}.

Now we focus on the lepton sector in the Yukawa part of Eq. (7). The normal lepton mass matrix M_e given in Eq. (10) is assumed to be diagonal for simplicity. As a result, the flavor basis of the charged leptons e'_a is the mass basis $e_{aL,R} \equiv e'_{aL,R}$, namely,

$$m_{e_a} = Y^e_{ab}\delta_{ab}\frac{v_1}{\sqrt{2}} \Rightarrow Y^e_{ab} = \delta_{ab}\frac{\sqrt{2}m_{e_a}}{v_1}. \tag{11}$$

Three other bases $f'_{L,R} \equiv (f'_1, f'_2, f'_3)^T_{L,R}$ with $f = \nu, E, N$ are transformed into the corresponding mass base $f'_{L,R}$ through the following relations:

$$U^{f\dagger}_L M_\nu U^f_R = \hat{M}_f = \text{diag}(m_{f_1}, m_{f_2}, m_{f_3}),\ \ f'_{L,R} = U^f_{L,R} f_{L,R}. \tag{12}$$

Although the quark sector is irrelevant to our work, we review here the main property relating to the recent experimental constraints of $K^0 - \bar{K}^0$ oscillation, similar to the 3-3-1 models [90,91]. The quark sector consists of two families of left-handed anti-quadruplets, one family

of a left-handed quadruplet, and singlets of right-handed quarks, namely,

$$Q_{3L} = \left(u'_3, d'_3, D'_3, U'_3\right)^T_L \sim \left(3, 4, \frac{1}{6}\right),\ Q_{\alpha L} = \left(d_\alpha, -u_\alpha, U'_\alpha, D'_\alpha\right)^T_L \sim \left(3, 4^*, \frac{1}{6}\right),\ \alpha = 1, 2,$$
$$u'_{iR} \sim (3, 1, 2/3),\ d'_{iR} \sim (3, 1, -1/3),\ D'_{iR} \sim (3, 1, -1/3),\ U'_{iR} \sim (3, 1, 2/3),\ i = \overline{1, 3}. \quad (13)$$

The relevant Yukawa parts of quarks respecting all gauge and $\mathcal{L}$ symmetries are

$$\begin{aligned} -\mathcal{L}^q_Y = &\sum_{i=1}^{3}\left[\sum_{\alpha=1}^{2}\left(Y^u_{\alpha i}\overline{Q_{\alpha L}}\rho^* u_{iR} + Y^d_{\alpha i}\overline{Q_{\alpha L}}\eta^* d_{iR}\right) + \left(Y^u_{3i}\overline{Q_{3L}}\eta u_{iR} + Y^d_{3i}\overline{Q_{3L}}\rho d_{iR}\right)\right] \\ &+ \sum_{\alpha,\beta=1}^{2}\left[Y^U_{\alpha\beta}\overline{Q_{\alpha L}}\phi^* U_{\beta R} + Y^D_{\alpha\beta}\overline{Q_{\alpha L}}\chi^* D'_{\beta R}\right] + Y^U_{33}\overline{Q_{3L}}\chi U_{\beta R} + Y^D_{33}\overline{Q_{3L}}\eta D'_{\beta R} \\ &+ \text{H.c.}. \end{aligned} \quad (14)$$

We can see that the Yukawa parts generating SM quark masses are the same as those shown in Refs. [90,91] for 3-3-1 models with right-handed neutrinos, where both ρ and χ inherit the same VEV properties. In addition, all exotic quarks do not mix with the SM quarks, consistent with the property shown in Table 2 that all SM quarks have zero L, in contrast with $L = \pm 2$ for all exotic quarks. Therefore, the couplings of the SM quarks with Higgs bosons in the models given in Refs. [90,91] are the same as those presented in the model under consideration. Accordingly, the mass split value Δm_K originated from the K^0-$\bar{K}^0$ oscillation predicted by the 3-4-1 model under consideration will be the sum of the new heavy Higgs and neutral gauge contributions at the tree level, in which every contribution is proportional to the inverse of the squared mass of the respective Higgs or gauge boson. As we will see below, the 3-4-1 model predicts two new heavy neutral gauge bosons Z_3 and Z_4 with masses $m^2_{Z_3} \propto w^2$ and $m^2_{Z_4} \propto V^2$ in the limit $V \gg w$. Because w plays the role of the $SU(3)_L$ scale, Ref. [90] confirms that if $m_{Z_4} \gg m_{Z_3} > 4$ TeV, contributions from these two gauge bosons to Δm_K will satisfy the experimental constraint. The case of the heavy Higgs contributions is the same. Because this choice of parameters does not affect the main results in our work, this experimental constraint will be ignored in the remaining part of this work.

2.2. *Gauge boson masses and mixing*

Gauge boson masses arise from the covariant kinetic term of Higgs multiplets, namely,

$$L_{\text{Higgs}} = \sum_{H}^{4}\left(D^\mu\langle H\rangle\right)^\dagger D_\mu\langle H\rangle, \quad (15)$$

where $H = \chi, \phi, \eta, \rho$. The covariant derivative is defined as

$$D_\mu = \partial_\mu - ig\sum_{a=1}^{15} W_{a\mu}T_a - ig_X X B''_\mu T_{16} \equiv \partial_\mu - igP^{NC}_\mu - igP^{CC}_\mu, \quad (16)$$

where g, g_X and $W_{a\mu}, B''_\mu$ are gauge couplings and fields of the gauge groups $SU(4)_L$ and $U(1)_X$, respectively. The two parts P^{NC}_μ and P^{CC}_μ relate to the neutral and non-hermitian currents [11]. For the quadruplet, $T_{16} = \frac{1}{2\sqrt{2}}\text{diag}(1, 1, 1, 1)$ and

$$P^{CC}_\mu = \frac{1}{\sqrt{2}}\begin{pmatrix} 0 & W^+ & W^+_{13} & W^0_{14} \\ W^- & 0 & W^0_{23} & W^-_{24} \\ W^-_{13} & W^{0*}_{23} & 0 & W^-_{34} \\ W^{0*}_{14} & W^+_{24} & W^+_{34} & 0 \end{pmatrix}_\mu, \quad (17)$$

where $t \equiv g_X/g$ and $\sqrt{2}\, W^{\mu}_{ij} \equiv W^{\mu}_{i} - iW^{\mu}_{j}$ with $i < j$. The upper subscripts label the electric charges of gauge bosons. The relation between the original basis (W_3, W_8, W_{15}, B'') and the mass basis (A, Z, Z_3, Z_4) of all real neutral bosons was determined previously [11]. The masses of non-Hermitian (charged) gauge bosons are given by

$$m^2_W = \frac{g^2\left(v_1^2+v_2^2\right)}{4}, m^2_{W_{13}} = \frac{g^2\left(v_2^2+\omega^2\right)}{4}, m^2_{W_{23}} = \frac{g^2\left(v_1^2+\omega^2\right)}{4},$$
$$m^2_{W_{14}} = \frac{g^2\left(v_2^2+V^2\right)}{4}, m^2_{W_{24}} = \frac{g^2\left(v_1^2+V^2\right)}{4}, m^2_{W_{34}} = \frac{g^2\left(\omega^2+V^2\right)}{4}. \tag{18}$$

By spontaneous symmetry breaking (SSB), the following relation should be in order: $V \gg \omega \gg v_1, v_2$. A consequence from Eq. (18) is that $W^{\pm}$ must be identified with the singly charged SM gauge boson, namely,

$$v_1^2 + v_2^2 = v^2 = 246^2\ \text{GeV}^2. \tag{19}$$

Then neutral gauge boson masses are

$$m^2_Z \simeq \frac{m^2_W}{c^2_W},\ m^2_{Z_3} \simeq \frac{4g^2c^2_W w^2}{3\left(1-4s^2_W\right)},\ m^2_{Z_4} \simeq \frac{g^2(9V^2+w^2)}{6}. \tag{20}$$

The above formula implies that η and ρ play roles as two Higgs doublets in the well-known two Higgs doublet models after the breaking steps to the SM gauge group $SU(2)_L \times U(1)_Y$. Then we define the mixing angle β as follows:

$$t_\beta \equiv \tan\beta = \frac{v_2}{v_1},\ v_1 = vc_\beta,\ v_2 = vs_\beta, \tag{21}$$

where $t_\beta \geq 0.4$ as the perturbative limit of the top quark Yukawa coupling $|Y^u_{33}| \simeq \sqrt{2}m_t/(vs_\beta) < \sqrt{4\pi}$. The upper bound of t_β may come from the tau mass $Y^\tau \simeq \sqrt{2}m_\tau/(vc_\beta) < \sqrt{4\pi}$, equivalently $t_\beta < 390$.

The mixing parameters of the neutral gauge bosons are summarized in Appendix B, see the details in Ref. [11]. Because the current study [90] shows that the breaking scale of $SU(3)_L$ and $SU(L)_L$ is on the order of TeV, the mixing parameters between Z, Z_3, and Z_4 are very small, therefore we ignore them in this work. But the loop corrections to the $Z\mu^+\mu^-$ may be significant, especially in the model inheriting the "chiral enhancement" enough to accommodate the $(g-2)_{e_a}$ anomaly data. These one-loop corrections are computed in Appendix B and used to constrain the experimental data in the numerical investigation.

2.3. *Higgs potential and Higgs spectrum*

The most general Higgs potential including the appearance of the singly charged Higgs boson $\sigma^{\pm} \sim (1, 1, \pm 1)$ is:

$$
\begin{aligned}
V_h &= V(\eta,\rho,\phi,\chi)+V(\sigma^{\pm}),\\
V(\eta,\rho,\phi,\chi) &= \mu_1^2\eta^\dagger\eta+\mu_2^2\rho^\dagger\rho+\mu_3^2\phi^\dagger\phi+\mu_4^2\chi^\dagger\chi\\
&\quad+\lambda_1(\eta^\dagger\eta)^2+\lambda_2(\rho^\dagger\rho)^2+\lambda_3(\phi^\dagger\phi)^2+\lambda_4(\chi^\dagger\chi)^2\\
&\quad+(\eta^\dagger\eta)[\lambda_5(\rho^\dagger\rho)+\lambda_6(\phi^\dagger\phi)+\lambda_7(\chi^\dagger\chi)]\\
&\quad+(\rho^\dagger\rho)[\lambda_8(\phi^\dagger\phi)+\lambda_9(\chi^\dagger\chi)]+\lambda_9'(\phi^\dagger\phi)(\chi^\dagger\chi)\\
&\quad+\lambda_{10}(\rho^\dagger\eta)(\eta^\dagger\rho)+\lambda_{11}(\rho^\dagger\phi)(\phi^\dagger\rho)+\lambda_{12}(\rho^\dagger\chi)(\chi^\dagger\rho)\\
&\quad+\lambda_{13}(\phi^\dagger\eta)(\eta^\dagger\phi)+\lambda_{14}(\chi^\dagger\eta)(\eta^\dagger\chi)+\lambda_{15}(\chi^\dagger\phi)(\phi^\dagger\chi)\\
&\quad+(f\epsilon^{ijkl}\eta_i\rho_j\phi_k\chi_l+\text{H.c.}),
\end{aligned}
\tag{22}
$$

$$
\begin{aligned}
V(\sigma^{\pm}) &= \mu_5^2\sigma^+\sigma^-+\lambda_\sigma\left(\sigma^+\sigma^-\right)^2+\left(f_\sigma\sigma^+\rho^\dagger\eta+\text{H.c.}\right)\\
&\quad+(\sigma^+\sigma^-)\left(\lambda_{\sigma\eta}\eta^\dagger\eta+\lambda_{\sigma\rho}\rho^\dagger\rho+\lambda_{\sigma\phi}\phi^\dagger\phi+\lambda_{\sigma\chi}\chi^\dagger\chi\right).
\end{aligned}
\tag{23}
$$

Here we consider the Higgs potential respecting the generalized lepton number $\mathcal{L}$ and the new singly charged Higgs boson has $\mathcal{L}(\sigma^{\pm})=0$. We also ignore the triple Higgs self-couplings $(f_\sigma'\chi^\dagger\phi+\text{h.c.})$ because these result in unnecessary mixing in our calculation. The detailed discussion to derive the masses and mixing parameters of the Higgs bosons was presented previously in Ref. [11] without $\sigma^{\pm}$. The Higgs potential consisting of $\sigma^{\pm}$ was discussed in 3-3-1 models [14,94], in which the detailed calculation to derive Higgs masses and mixing was performed. We collect only the most important results relating to our work.

The mixing of $\chi_2^{\pm}$ and $\rho_4^{\pm}$ results in two massless Goldstone bosons $G_{24}^{\pm}$ and two singly charged Higgs bosons $h_3^{\pm}$:

$$
\begin{pmatrix}\chi_2^{\pm}\\ \rho_4^{\pm}\end{pmatrix}=\begin{pmatrix}c_{\theta_1} & s_{\theta_1}\\ -s_{\theta_1} & c_{\theta_1}\end{pmatrix}\begin{pmatrix}G_{24}^{\pm}\\ h_3^{\pm}\end{pmatrix},\ M_{h_3^+}^2=\left({c_\beta}^2v^2+V^2\right)\left(\frac{\lambda_{12}}{2}-\frac{ft_\beta w}{2V}\right),
\tag{24}
$$

and

$$
s_{\theta 1}\equiv\sin\theta_1,\ c_{\theta 1}\equiv\cos\theta_1,\ \tan\theta_1=\frac{vc_\beta}{V}.
\tag{25}
$$

We consider here the mixing of ϕ_2^{0*} and ρ_3^0, which leads to a non-hermitian Goldstone boson $G_{23}^0\neq G_{23}^{0*}$ and a physical state $H_1^0\neq H_1^{0*}$

$$
\begin{pmatrix}\phi_2^{0*}\\ \rho_3^0\end{pmatrix}=\begin{pmatrix}c_{\theta_2} & s_{\theta_2}\\ -s_{\theta_2} & c_{\theta_2}\end{pmatrix}\begin{pmatrix}G_{23}^0\\ H_1^0\end{pmatrix},\ M_{H_1^0}^2=\left({c_\beta}^2v^2+w^2\right)\left(\frac{\lambda_{11}}{2}-\frac{ft_\beta V}{2w}\right),
\tag{26}
$$

and

$$
s_{\theta_2}\equiv\sin\theta_2,\ c_{\theta_2}\equiv\cos\theta_2,\ \tan\theta_2=\frac{vc_\beta}{w}.
\tag{27}
$$

Three singly charged Higgs bosons $(\rho_1^{\pm},\ \eta_2^{\pm},\sigma^{\pm})$ are changed into the two physical states $h_{1,2}^{\pm}$ and the Goldstone bosons $G_W^{\pm}$ of $W^{\pm}$ as follows:

$$
\begin{aligned}
\rho_1^{\pm} &= c_\beta\phi_W^{\pm}+s_\beta\left(c_\alpha h_1^{\pm}+s_\alpha h_2^{\pm}\right),\\
\eta_2^{\pm} &= -s_\beta\phi_W^{\pm}+c_\beta\left(c_\alpha h_1^{\pm}+s_\alpha h_2^{\pm}\right),\\
\sigma^{\pm} &= -s_\alpha h_1^{\pm}+c_\alpha h_2^{\pm}.
\end{aligned}
\tag{28}
$$

The relations in Eq. (28) were given in Refs. [14,94], and consist of the same part $V(\sigma)$ given in Eq. (23) in the Higgs potential. The mixing parameter α and Higgs boson masses $m_{h_1^+}, m_{h_2^+}$ will

be investigated as free parameters, while three dependent parameters are:

$$\begin{aligned}
\mu_5^2 &= c_\alpha{}^2 m_{h_2^+}^2 + s_\alpha{}^2 m_{h_1^+}^2 - \frac{1}{2}\left(c_\beta{}^2 \lambda_{\sigma\rho} v^2 + \lambda_{\sigma\chi} V^2 + \lambda_{\sigma\phi} w^2 + \lambda_{\sigma\eta} s_\beta{}^2 v^2\right), \\
f &= -\frac{c_\beta s_\beta \left(2c_\alpha{}^2 m_{h_1^+}^2 - \lambda_{10} v^2 + 2 s_\alpha{}^2 m_{h_2^+}^2\right)}{V w}, \\
f_\sigma &= -\frac{\sqrt{2} c_\alpha s_\alpha \left(m_{h_1^+}^2 - m_{h_2^+}^2\right)}{v}.
\end{aligned} \tag{29}$$

As usual, this model must contain an SM-like Higgs boson confirmed by the LHC. A detailed calculation to identify this Higgs boson in the model under consideration can be found in Ref. [11]. A simple estimation is presented in Appendix A. In general, the SM-like Higgs boson gets its main contributions from η and ρ, similarly to the case of the property of the well-known two Higgs doublet model (2HDM). In the model under consideration, the flavor and the physical base of charged leptons are the same, as assumed in Eq. (11). As a result, there is no mixing between SM and heavy charged leptons, implying that the leading corrections to the SM coupling $h\mu^+\mu^-$ are the combination of the tree level of the Higgs mixing and the one-loop level [95–98]. As commented in Ref. [95], the recent experiments give no hint for $h \to e^+e^-$, while only evidence of $h \to \mu^+\mu^-$ was reported [99,100]. The loop corrections to the coupling $h\mu^+\mu^-$ are smaller than the recent experimental sensitivities, but may be detected in the future [95–97]. Therefore, the constraint from the modification of the coupling $h\mu^+\mu^-$ will not affect the allowed regions of the parameter space we will discuss in this work.

2.4. *Analytic formulas for one-loop contributions to a_{e_a} with active Dirac neutrinos*

In this section, we consider the simple case that $\nu_{1,2,3}$ are Dirac ones, and no mixing between $\sigma^\pm$ and other singly charged Higgs bosons, i.e. $s_\alpha = 0$, $c_\alpha = 1$, then only $h_2^\pm$ couples with active neutrinos. The conclusion with $s_\alpha \neq 0$ is unchanged because the tiny neutrino masses result in suppressed one-loop contributions to $(g-2)_{e_a}$ anomalies.

The relevant Lagrangian giving one-loop contributions to a_{e_a} is:

$$\begin{aligned}
-\mathcal{L}_y^l = &\frac{g}{\sqrt{2} m_{W_{23}}} \sum_{a,c=1}^{3} U_{L,ac}^{E*} \left[m_{E_c} t_{\theta_2} P_L + m_{e_a} t_{\theta_2}^{-1} P_R\right] e_a H_1^0 \\
&+ \frac{g}{\sqrt{2} m_{W_{24}}} \sum_{a,c=1}^{3} U_{L,ac}^{N*} \left[m_{N_c} t_{\theta_1} P_L + m_{e_a} t_{\theta_1}^{-1} P_R\right] e_a h_3^+ \\
&+ \frac{g}{\sqrt{2} m_W} \sum_{a,c=1}^{3} \overline{\nu_c} U_{L,ac}^{\nu*} \left(m_{\nu_c} t_\beta^{-1} P_L + m_{e_a} t_\beta P_R\right) e_a h_1^+ + \text{H.c.} + \ldots .
\end{aligned} \tag{30}$$

To avoid large cLFV decays $e_b \to e_a \gamma$, which may be ruled out by experiments, we will pay attention to the limit that $U_L^N = U_L^E = I_3$, and $m_{E_a} = m_E, m_{N_a} = m_N$ for all $a = 1, 2, 3$. For active neutrinos having tiny masses, the respective one-loop contributions to Δa_{e_a} are suppressed. The

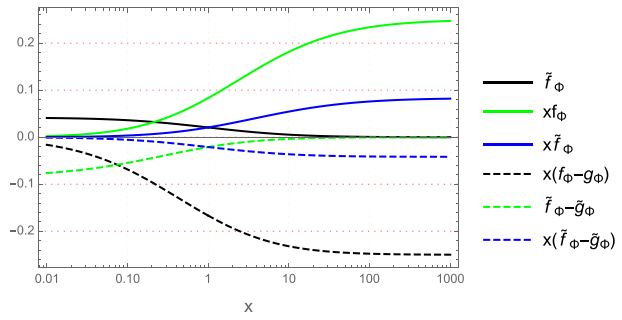

Fig. 1. Properties of the scalar functions relating to one-loop contributions of heavy Higgs bosons to $(g-2)_{e_a}$ anomalies in the 3-4-1 model with active Dirac neutrinos.

relevant non-zero form factors with one-loop contributions to a_{e_a} are [19]:

$$
\begin{aligned}
a_{e_a}(h_3^+) &= -\frac{g^2 m_{e_a}^2}{8\pi^2 m_W^2}\left\{\frac{v^2}{V^2}\times x_N f_\Phi(x_N) + \left[\frac{v^4 c_\beta^2}{V^4}x_N + \frac{m_{e_a}^2 c_{\theta_1}^2}{m_{h_3^+}^2 c_\beta^2}\right]\tilde{f}_\Phi(x_N)\right\},\\
a_{e_a}(h_1^+) &= -\frac{g^2 m_{e_a}^2}{8\pi^2 m_W^2}\left(\frac{m_{e_a} t_\beta}{m_{h_1^+}}\right)^2 \tilde{f}_\Phi(0),\\
a_{e_a}(H_1^0) &= -\frac{g^2 m_{e_a}^2}{8\pi^2 m_W^2}\left\{\frac{v^2}{w^2}x_E\left[f_\Phi(x_E) - g_\Phi(x_E)\right] + \left(\frac{v^4 s_\beta^2}{w^4}x_E + \frac{m_{e_a}^2 c_{\theta_2}^2}{m_{H_1^0}^2 c_\beta^2}\right)\left[\tilde{f}_\Phi(x_E) - \tilde{g}_\Phi(x_E)\right]\right\},
\end{aligned}
\tag{31}
$$

where $x_N = m_N^2/m_{h_3^+}^2$ and $x_E = m_E^2/m_{H_1^0}^2$, and

$$
\begin{aligned}
f_\Phi(x) = 2\tilde{g}_\Phi(x) &= \frac{x^2 - 1 - 2x\ln x}{4(x-1)^3},\\
g_\Phi &= \frac{x - 1 - \ln x}{2(x-1)^2},\\
\tilde{f}_\Phi(x) &= \frac{2x^3 + 3x^2 - 6x + 1 - 6x^2\ln x}{24(x-1)^4}.
\end{aligned}
\tag{32}
$$

The total contribution to Δa_{e_a} from all Higgs bosons is:

$$
a_{e_a}(H) = \sum_X a_{e_a}(X), \tag{33}
$$

where $X = h_1^+, h_3^+, H_1^0$.

The functions relating to one-loop contributions of Higgs bosons are shown in Fig. 1. Because $xf_\Phi(x)$, $\tilde{f}_\Phi(x)$, $x\tilde{f}_\Phi(x) > 0$ for all $x > 0$, the one-loop contributions from singly charged Higgs bosons $h_{1,3}^\pm$ are in opposite signs to $\Delta a_\mu^{\rm NP}$, hence they should be small. On the other hand, the one-loop contribution from the neutral Higgs boson H_1^0 consists of negative functions $(f_\Phi(x) - g_\Phi(x))$, and $\left(\tilde{f}_\Phi(x) - \tilde{g}_\Phi(x)\right)$, hence the final contributions support large Δa_μ.

The couplings of leptons and non-hermitian gauge bosons are

$$
\begin{aligned}
\mathcal{L}^{\ell\ell V} &= i\overline{L_{aL}}\gamma^\mu D_\mu L_{aL}\\
&= \frac{g}{\sqrt{2}}\left[U_{ai}^{\nu *}\overline{\nu_i}\gamma^\mu P_L e_a W_\mu^+ + U_{ai}^{N*}\overline{N_i}\gamma^\mu P_L e_a W_{24\mu}^+ + \overline{e_{aL}}\gamma^\mu E'_{aL}W_{23\mu}^0 + \ldots,\right]\\
&\quad + \text{H.c.},
\end{aligned}
\tag{34}
$$

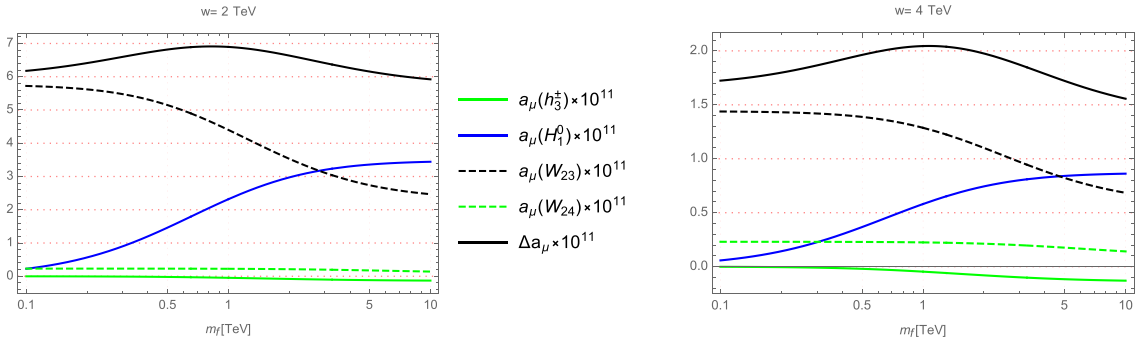

Fig. 2. One-loop contributions of new $SU(4)_L$ particles to a_μ with $w = 2$ TeV (left panel) and $w = 4$ TeV (right panel).

where the last line collects only terms giving one-loop contributions to cLFV amplitudes and $(g-2)$ anomalies, resulting in the following formulas [19]:

$$a_{e_a}(W) = -\frac{g^2 m_{e_a}^2}{8\pi^2 m_W^2}\sum_{i=1}^{3} U_{ai}^{\nu} U_{ai}^{\nu *}\tilde{f}_V\left(x_{\nu_i}\right) \simeq -\frac{g^2 m_{e_a}^2}{8\pi^2 m_W^2}\tilde{f}_V\left(0\right), \tag{35}$$

$$a_{e_a}(W_{24}) = -\frac{g^2 m_{e_a}^2}{8\pi^2 m_W^2}\sum_{b=1}^{3} U_{ab}^{N} U_{ab}^{N*}\frac{m_W^2}{m_{W_{24}}^2}\tilde{f}_V\left(x_{N_b}\right) = -\frac{g^2 m_{e_a}^2}{8\pi^2 m_W^2}\times\frac{m_W^2}{m_{W_{24}}^2}\tilde{f}_V\left(x_N\right), \tag{36}$$

$$a_{e_a}(W_{23}) = -\frac{g^2 m_{e_a}^2}{8\pi^2 m_W^2}\sum_{b=1}^{3} U_{ab}^{E} U_{ab}^{E*}\frac{m_W^2}{m_{W_{23}}^2}\tilde{f}_V\left(x_{E_b}\right) = -\frac{g^2 m_{e_a}^2}{8\pi^2 m_W^2}\times\frac{m_W^2}{m_{W_{23}}^2}\tilde{f}_V\left(x_E\right), \tag{37}$$

where

$$\tilde{f}_V(x) = \frac{-4x^4 + 49x^3 - 78x^2 + 43x - 10 - 18x^3\ln x}{24(x-1)^4}. \tag{38}$$

The total contribution from new heavy gauge bosons to the a_{e_a} is

$$a_{e_a}(V) = a_{e_a}(W_{23}) + a_{e_a}(W_{24}). \tag{39}$$

The deviation of a_μ between predictions by the two models 3-4-1 and SM is

$$\Delta a_{e_a}^{341} \equiv \Delta a_{e_a} = \Delta a_{e_a}(W) + a_{e_a}(V) + a_{e_a}(H), \quad \Delta a_{e_a}^{W} = a_{e_a}^{W} - a_{e_a}^{\rm SM}(W), \tag{40}$$

where $a_\mu^{\rm SM}(W) = 3.887\times10^{-9}$ [101], and $a_{e_a}^{\rm SM}(W) = a_\mu^{\rm SM}(W)\times(m_{e_a}^2/m_\mu^2)$ is the SM's prediction for the one-loop contribution from the W boson. In this work, $\Delta a_{e_a}^{341} = \Delta a_{e_a}$ will be considered as new physics (NP) predicted by the 3-4-1 models, which must satisfy the experimental data given in Eqs. (1) and (2) in the numerical investigation.

Numerical illustrations are shown in Fig. 1 with fixed $w = 5$ TeV, $V = 10$ TeV, $m_{h_1^\pm} = m_{h_3^\pm} = m_{H_1^0} = 1$ TeV, and $t_\beta = 50$. Different contributions are considered as functions of $m_N = m_E = m_f$ with numerical illustrations given in Fig. 2. Both $a_{e_a}(W)$ and $a_{e_a}(h_1^\pm)$ are independent with m_f, w, and V. In addition, the one-loop contribution from the $W^\pm$ gauge boson is $a_{e_a}(W) = a_{e_a}^{\rm SM}(W)$, hence it does not affect Δa_μ. The two conditions $t_\beta \leq 100$ and $m_{h_1^\pm} \geq 200$ GeV give $0 < a_\mu(h_1^+) \leq 10^{-12}$, hence $a_\mu(h_1^+)$ gives suppressed contributions to Δa_μ. The Δa_μ depends strongly on w, which lower bound is constrained strictly from the masses, which are given in Eq. (20), of heavy neutral gauge bosons $Z_{3,4}$, namely $m_{Z_{3,4}} > 3$ TeV from LHC searches [18]. As a result, large values of $w \geq 2$ TeV give $\Delta a_\mu \leq 7\times10^{-13} \ll 192\times10^{-13} \leq a_\mu^{\rm NP}$. In conclusion, all the one-loop contributions mentioned above are much smaller than $a_\mu^{\rm NP}$.

3. The 341ISS with ISS neutrinos

Now we consider an extension of the above 341RHN model that may explain successfully the $(g-2)_{e_a}$ data. This version consists of six right-handed neutrinos ν_{aR}, $X_{aR} \sim (1, 0)$, $a = 1, 2, 3$ generating active neutrino masses through the ISS mechanism, and a singly charged Higgs boson $\sigma^+ \sim (1, 1, 1)$ needed to give large one-loop contributions to anomalous magnetic moment (AMM). We call this model the 3-4-1 model with ISS neutrinos (341ISS). The generalized lepton numbers are $\mathcal{L}(\nu_{aR}) = 1$, $\mathcal{L}(X_{aR}) = -1$, and $\mathcal{L}(\sigma^+) = 0$. Now tree-level neutrino masses and mixing angles arise from the ISS mechanism. Requiring that $\mathcal{L}$ is only softly broken, the additional Yukawa part is

$$-\mathcal{L}_{Y,\nu_R} = Y^{\nu}_{ab}\overline{\nu_{aR}}\eta^{\dagger}L_b + (M_R)_{ab}\overline{\nu_{aR}}(X_{bR})^c + \frac{1}{2}(\mu_X)_{ab}\overline{X_{aR}}(X_{bR})^c + Y^{\sigma}_{ab}\overline{(X_{aR})^c}e_{bR}\sigma^+ + \text{h.c.}, \tag{41}$$

where Y^{ν}, M_R, μ_X, and Y^{σ} are 3×3 matrices. The first term in Eq. (41) is similar to that given in Eq. (7), but it will generate the Dirac neutrino mass matrix M_D instead of the active neutrino masses.

Notations for flavor states of active left-handed neutrinos are $\nu_L = (\nu'_1, \nu'_2, \nu'_3)^T_L$ and $\nu_R = (\nu_1, \nu_2, \nu_3)^T_R$, $X_R = (X_1, X_2, X_3)^T_R$. The neutrino mass terms derived from Eq. (41) are written in the following ISS form [102]:

$$-\mathcal{L}^{\nu}_{\text{mass}} \equiv \frac{1}{2}\left(\overline{(\nu_L)^c},\ \overline{\nu_R},\ \overline{X_R}\right)\mathcal{M}^{\nu}\begin{pmatrix}\nu_L\\(\nu_R)^c\\(X_R)^c\end{pmatrix} + \text{h.c.},$$

$$\mathcal{M}^{\nu} = \begin{pmatrix}\mathcal{O}_{3\times3} & M_D^T\\ M_D & M_N\end{pmatrix},\ M_D = \begin{pmatrix}m_D\\ \mathcal{O}_{3\times3}\end{pmatrix},\ M_N = \begin{pmatrix}\mathcal{O}_{3\times3} & M_R\\ M_R^T & \mu_X\end{pmatrix}, \tag{42}$$

where $\mathcal{O}_{3\times3}$ is a zero matrix and $m_D = Y^{\nu} \times v_2/\sqrt{2}$. The analytic form of the Dirac mass matrix was chosen generally following Ref. [103].

The total unitary mixing matrix U^{ν} is defined as follows:

$$U^{\nu T}\mathcal{M}^{\nu}U^{\nu} = \hat{\mathcal{M}}^{\nu} = \text{diag}(m_{n_1}, m_{n_2}, m_{n_3}, m_{n_4}, ..., m_{n_9}) \equiv \text{diag}\left(\hat{m}_{\nu},\ \hat{M}_N\right), \tag{43}$$

where m_{n_i} $(i = 1, 2,..., 9)$ are eigenvalues of the nine mass eigenstates n_{iL}, including three light active neutrinos n_{aL} $(a = 1, 2, 3)$ with mass matrix $\hat{m}_{\nu}$ and six other heavy neutrinos with mass matrix $\hat{M}_N$. The relations between the flavor and mass eigenstates are

$$\begin{pmatrix}\nu_L\\(\nu_R)^c\\(X_R)^c\end{pmatrix} = U^{\nu}n_L, \quad \text{and} \quad \begin{pmatrix}(\nu_L)^c\\ \nu_R\\ X_R\end{pmatrix} = U^{\nu *}n_R, \tag{44}$$

where $n_L \equiv (n_{1L}, n_{2L},..., n_{9L})^T$ and $n_R = (n_L)^c$. The neutrino mixing matrix is parameterized in the following form:

$$U^{\nu} = \begin{pmatrix}\left(I_3 - \frac{1}{2}RR^{\dagger}\right)U_{\text{PMNS}} & RV\\ -R^{\dagger}U_{\text{PMNS}} & \left(I_6 - \frac{1}{2}R^{\dagger}R\right)V\end{pmatrix} + \mathcal{O}(R^3), \tag{45}$$

where U_{PMNS} is the 3×3 Pontecorvo–Maki–Nakagawa–Sakata (PMNS) matrix [104,105], V is a 6×6 unitary matrix, and R is a 3×6 matrix satisfying $|R_{aI}| \ll 1$ for all $a = 1, 2, 3$ and $I = 1, 2,..., 6$. In the ISS framework we considered here, m_D is parameterized in terms of many free parameters, hence it is convenient to choose a simple form of $\mu_X = \mu_0 I_3$ and $M_R = \hat{M}_R = M_0 I_3$

[106,107]. The formulas of m_D and mixing parameters are [103]:

$$m_D = M_0\sqrt{\hat{x}_\nu}U^\dagger_{\rm PMNS},\ R \simeq \left(0,\ U_{\rm PMNS}\hat{x}_\nu^{1/2}\right),\ \hat{x}_\nu \equiv \frac{\hat{m}_\nu}{\mu_0}, \tag{46}$$

where $\max[|(\hat{x}_\nu)_{aa}|] \ll 1$ for all $a = 1, 2, 3$.

The ISS conditions $|\hat{m}_\nu| \ll |\mu_0| \ll |m_D| \ll M_0$ so that $\frac{\sqrt{\mu_0\hat{m}_\nu}}{M_0} \simeq 0$, and the mixing matrix and Majorana mass term are

$$\hat{M}_N = \begin{pmatrix} \hat{M}_R & 0 \\ 0 & \hat{M}_R \end{pmatrix} \simeq M_0 I_6,\ V \simeq \frac{1}{\sqrt{2}}\begin{pmatrix} -iI_3 & I_3 \\ iI_3 & I_3 \end{pmatrix}, \tag{47}$$

which give $V^*\hat{M}_N V^\dagger \simeq M_N$, i.e. $m_{n_i} \simeq M_0$ for all $i = 4, 5,..., 9$.

3.1. *Analytic formulas for one-loop contributions to a_{e_a} and $Br(e_b \to e_a\gamma)$*

We note that except the contributions from ISS neutrino couplings with singly charged Higgs bosons given in Eq. (28), all other contributions are the same results as those discussed in the case of Dirac active neutrinos mentioned above. Hence, we just focus here on the Higgs contributions relating to the couplings with ISS neutrinos. The relevant couplings are listed in the following Lagrangian:

$$\mathcal{L} = -\frac{g}{\sqrt{2}m_W}\sum_{k=1}^{2}\sum_{a=1}^{3}\sum_{i=1}^{9}\overline{n_i}\left[\lambda^{L,k}_{ia}P_L + \lambda^{R,k}_{ia}P_R\right]e_a h^+_k + \sum_{a=1}^{3}\sum_{i=1}^{9}\frac{g}{\sqrt{2}}U^{\nu *}_{ai}\overline{n_i}\gamma^\mu P_L e_a W^+_\mu + \text{h.c.}, \tag{48}$$

where

$$\begin{aligned}
\lambda^{L,1}_{ia} &= \sum_{I=1}^{6} t_\beta^{-1} M_{D,Ia} c_\alpha U^\nu_{(I+3)i} \simeq \frac{t_\beta^{-1}c_\alpha}{\sqrt{2}} \times \begin{bmatrix} 0, & i \le 3 \\ -iM_0\left(U^*_{\rm PMNS}\hat{x}_\nu^{1/2}\right)_{a(i-3)} & 3 < i \le 6 \\ M_0\left(U^*_{\rm PMNS}\hat{x}_\nu^{1/2}\right)_{a(i-6)} & i \ge 7 \end{bmatrix}, \\
\lambda^{L,2}_{ia} &\simeq \lambda^{L,1}_{ia} t_\alpha, \\
\lambda^{R,1}_{ia} &= m_{e_a} t_\beta c_\alpha U^{\nu *}_{ai} - \sum_{I=1}^{6}\frac{v}{\sqrt{2}} s_\alpha Y^\sigma_{Ia} U^{\nu *}_{(I+3)i} \\
&\simeq \begin{bmatrix} m_{e_a} t_\beta c_\alpha \left[U^*_{\rm PMNS}\left(I_3 - \frac{1}{2}\hat{x}_\nu\right)\right]_{ai} + \frac{vs_\alpha}{\sqrt{2}}\left(Y^{\sigma T}\hat{x}_\nu^{1/2}\right)_{ai} & i \le 3 \\ \frac{-i}{\sqrt{2}} m_{e_a} t_\beta c_\alpha \left(U^*_{\rm PMNS}\hat{x}_\nu^{1/2}\right)_{a(i-3)} + \frac{ivs_\alpha}{2}\left[Y^{\sigma T}\left(I_3 - \frac{1}{2}\hat{x}_\nu\right)\right]_{a(i-3)} & 4 \le i < 7 \\ \frac{1}{\sqrt{2}} m_{e_a} t_\beta c_\alpha \left(U^*_{\rm PMNS}\hat{x}_\nu^{1/2}\right)_{a(i-6)} - \frac{vs_\alpha}{2}\left[Y^{\sigma T}\left(I_3 - \frac{1}{2}\hat{x}_\nu\right)\right]_{a(i-6)} & i \ge 7 \end{bmatrix}, \\
\lambda^{R,2}_{ia} &= \lambda^{R,1}_{ia}\left[s_\alpha \to -c_\alpha,\ c_\alpha \to s_\alpha\right].
\end{aligned} \tag{49}$$

The branching ratios of the cLFV decays are formulated as follows [19,108,109]:

$$\text{Br}(e_b \to e_a\gamma) = \frac{48\pi^2}{G_F^2 m_b^2}\left(\left|c_{(ab)R}\right|^2 + \left|c_{(ba)R}\right|^2\right)\text{Br}(e_b \to e_a\overline{\nu_a}\nu_b), \tag{50}$$

where $G_F = g^2/(4\sqrt{2}m_W^2)$, $\mathrm{Br}(\mu \to e\overline{\nu_e}\nu_\mu) \simeq 1$, $\mathrm{Br}(\tau \to e\overline{\nu_e}\nu_\tau) \simeq 0.1782$, $\mathrm{Br}(\tau \to \mu\overline{\nu_\mu}\nu_\tau) \simeq 0.1739$ [102], and

$$
\begin{aligned}
c_{(ab)R} &= \sum_{k=1}^{2} c_{(ab)R}\left(h^{\pm}\right) + c_{(ab)R}(W), \quad c_{(ba)R} = c_{(ab)R}[a \to b,\ b \to a], \\
c_{(ab)R}\left(h^{\pm}\right) &= \sum_{k=1}^{2} c_{(ab)R}\left(h_k^{\pm}\right), \\
c_{(ab)R}\left(h_k^{\pm}\right) &= \frac{g^2 e}{32\pi^2 m_W^2 m_{h_k^{\pm}}^2} \\
&\quad \times \sum_{i=1}^{9}\left[\lambda_{ia}^{L,k*}\lambda_{ib}^{R,k} m_{n_i} f_\Phi(x_{i,k}) + \left(m_{e_b}\lambda_{ia}^{L,k*}\lambda_{ib}^{L,k} + m_{e_a}\lambda_{ia}^{R,k*}\lambda_{ib}^{R,k}\right)\tilde{f}_\Phi(x_{i,k})\right], \quad (51)
\end{aligned}
$$

with $x_{i,k} \equiv m_{n_i}^2/m_{h_k^{\pm}}^2$.

Up to the order $\mathcal{O}(R^2)$ of the neutrino mixing matrix given in Eq. (45), the non-zero one-loop contributions relating to $h_{1,2}^{\pm}$ are:

$$
\begin{aligned}
c_{(ab)R}\left(h_1^{\pm}\right) &= \frac{eG_F m_{e_b}}{4\sqrt{2}\pi^2} \\
&\quad \times \left\{\left[c_\alpha^2\left(U_{\mathrm{PMNS}}\hat{x}_\nu U_{\mathrm{PMNS}}^{\dagger}\right)_{ab} - \frac{v t_\beta^{-1} c_\alpha s_\alpha}{m_{e_b}\sqrt{2}}\left(U_{\mathrm{PMNS}}\hat{x}_\nu^{1/2} Y^\sigma\right)_{ab}\right] x_1 f_\Phi(x_1)\right. \\
&\quad + t_\beta^{-2} c_\alpha^2\left(U_{\mathrm{PMNS}}\hat{x}_\nu U_{\mathrm{PMNS}}^{\dagger}\right)_{ab} x_1 \tilde{f}_\Phi(x_1) \\
&\quad + \frac{m_{e_a}^2 t_\beta^2 c_\alpha^2}{m_{h_1^{\pm}}^2}\left[\frac{\delta_{ab}}{24} - \left(U_{\mathrm{PMNS}}\hat{x}_\nu U_{\mathrm{PMNS}}^{\dagger}\right)_{ab}\left(\frac{1}{24} - \tilde{f}_\Phi(x_1)\right)\right] \\
&\quad + \frac{m_{e_a} v^2 s_\alpha^2}{2 m_{e_b} m_{h_1^{\pm}}^2}\left[\left(Y^{\sigma\dagger}\hat{x}_\nu Y^\sigma\right)_{ab}\left(\frac{1}{24} - \tilde{f}_\Phi(x_1)\right) + \left(Y^{\sigma\dagger}Y^\sigma\right)_{ab}\tilde{f}_\Phi(x_1)\right] \\
&\quad \left. + \frac{v m_{e_a} t_\beta s_{2\alpha}}{2\sqrt{2} m_{h_1^{\pm}}^2}\left(\frac{1}{24} - \tilde{f}_\Phi(x_1)\right)\left[\frac{m_{e_a}}{m_{e_b}}\left(U_{\mathrm{PMNS}}\hat{x}_\nu^{1/2} Y^\sigma\right)_{ab} + \left(U_{\mathrm{PMNS}}\hat{x}_\nu^{1/2} Y^\sigma\right)_{ba}^{*}\right]\right\}, \\
c_{(ab)R}(h_2^{\pm}) &= c_{(ab)R}(h_1^{\pm})[x_1 \to x_2,\ s_\alpha \to -c_\alpha,\ c_\alpha \to s_\alpha], \\
c_{(ab)R}(W) &\simeq \frac{eG_F m_{e_b}}{4\sqrt{2}\pi^2}\left[-\frac{5\delta_{ab}}{12} + \left(U_{\mathrm{PMNS}}\hat{x}_\nu U_{\mathrm{PMNS}}^{\dagger}\right)_{ab} \times \left(\tilde{f}_V(x_W) + \frac{5}{12}\right)\right]. \quad (52)
\end{aligned}
$$

The one-loop contributions from the $h_{1,2}^{\pm}$ exchanges to a_{e_a} are:

$$
\begin{aligned}
a_{e_a}\left(h_1^{\pm}\right) &= -\frac{4m_{e_a}}{e}\mathrm{Re}[c_{(aa)R}(h_1^{\pm})], \\
a_{e_a}\left(h_2^{\pm}\right) &= a_\mu(h_1^{\pm})[x_1 \to x_2,\ s_\alpha \to -c_\alpha,\ c_\alpha \to s_\alpha], \\
a_{e_a}(h^{\pm}) &= a_{e_a}(h_1^{\pm}) + a_{e_a}(h_2^{\pm}), \quad (53)
\end{aligned}
$$

where $x_k = M_0^2/m_{h_k^{\pm}}^2$ and $a_{e_a}(h^{\pm})$ is the total contribution from these two Higgs bosons. We note that all Yukawa couplings considered in this work are assumed to be real. As a result, Eq. (52) shows that only the Dirac phase results in the tiny values of $\mathrm{Im}[c_{aa}]$, implying very suppressed values of electric dipole moments $d_{e_a} \equiv -2\,\mathrm{Im}[c_{aa}]$ [19], consistent with experimental

constraints [110,111]. This conclusion is also confirmed by our numerical investigation, namely $|d_{e,\mu}| < 10^{-44}[e\,\text{cm}]$, therefore we will not discuss it further.

For qualitative estimation, the main contribution to $a_{e_a}(h^\pm)$ is the chirally enhanced part [19]. From Eq. (52), this part is determined as follows:

$$a_{e_a,0} = \frac{G_F m_{e_a}^2}{\sqrt{2}\pi^2} \times \text{Re}\left\{\left[\frac{v t_\beta^{-1} c_\alpha s_\alpha}{\sqrt{2} m_{e_a}} U_{\text{PMNS}} \hat{x}_\nu^{1/2} Y^\sigma\right]_{aa} [x_1 f_\Phi(x_1) - x_2 f_\Phi(x_2)]\right\}. \tag{54}$$

But this term may also give large contributions to $c_{(ab)R}$ and $c_{(ba)R}$, which may be excluded by the cLFV constraints with $b \neq a$. To avoid this problem, we start from the diagonal form of $c_{(ab)R,\,0}$ as follows:

$$c_{(ab)R,0} \propto \left[U_{\text{PMNS}} \hat{x}_\nu^{1/2} Y^\sigma\right]_{ab} \propto \delta_{ab}. \tag{55}$$

Correspondingly, the formula of $a_{e_a,0}$ is proportional to a diagonal matrix Y^d satisfying:

$$U_{\text{PMNS}} \times \text{diag}\left(\frac{m_{n_1}}{m_{n_3}}, \frac{m_{n_2}}{m_{n_3}}, 1\right)^{1/2} Y^\sigma = Y^d \equiv \text{diag}\left(Y_{11}^d, Y_{22}^d, Y_{33}^d\right). \tag{56}$$

Hence, the diagonal entries will give main contributions to a_{e_a}, namely,

$$a_{e_a,0} = \frac{G_F m_{e_a}^2 \sqrt{x_0}}{\sqrt{2}\pi^2} \times \text{Re}\left[\frac{v t_\beta^{-1} c_\alpha s_\alpha}{\sqrt{2} m_{e_a}} Y^d\right]_{aa} [x_1 f_\Phi(x_1) - x_2 f_\Phi(x_2)]. \tag{57}$$

Then $a_{e_a,0}$ may be large, provided that t_β should not be too large, $t_1 \neq t_2$, and the following quantities are large enough: x_0, $|s_{2\alpha} = 2 s_\alpha c_\alpha|$, and $|Y_{aa}^d|$ with $a = 1, 2, 3$. In contrast, cLFV amplitudes do not get any contributions from $c_{(ab)R,\,0}$. Numerical investigations will be done to check this conclusion. For simplicity, we use the approximation that all tiny contributions are ignored in the numerical results. Namely, $\Delta a_{e_a} \equiv a_{e_a}(h^\pm)$ given in Eq. (52), instead of the total formula given in Eq. (40). In contrast, the one-loop contribution from W must be included in the formulas of $\text{Br}(e_b \to e_a \gamma)$. This conclusion was confirmed based on the qualitative estimation discussed above. The numerical checks have been performed, which are consistent with previous discussions on 3-3-1 models [112,113].

Although our numerical investigation will consider only the experimental constraint given in Eq. (2) allowing only positive values of Δa_e^{NP} around 1σ constraint, the experimental result with negative Δa_e^{NP} in Ref. [75] can be explained similarly because the sign of the main contribution in Eq. (57) depends precisely on the signs of $Y^d s_\alpha c_\alpha$.

4. Numerical discussion

We will use the best-fit values of the neutrino oscillation data [102] corresponding to the normal order (NO) scheme with $m_{n_1} < m_{n_2} < m_{n_3}$, namely,

$$\begin{aligned} &s_{12}^2 = 0.32,\ s_{23}^2 = 0.547,\ s_{13}^2 = 0.0216,\ \delta = 218\ [\text{Deg}], \\ &\Delta m_{21}^2 = 7.55 \times 10^{-5}[\text{eV}^2],\ \Delta m_{32}^2 = 2.424 \times 10^{-3}[\text{eV}^2]. \end{aligned} \tag{58}$$

The active mixing matrix and neutrino masses are determined as follows:

$$\begin{aligned} \hat{m}_\nu &= \left(\hat{m}_\nu^2\right)^{1/2} = \text{diag}\left(m_{n_1}, \sqrt{m_{n_1}^2 + \Delta m_{21}^2}, \sqrt{m_{n_1}^2 + \Delta m_{21}^2 + \Delta m_{32}^2}\right), \\ U_{\text{PMNS}} &= \begin{pmatrix} c_{12}c_{13} & c_{13}s_{12} & s_{13}e^{-i\delta} \\ -c_{23}s_{12} - c_{12}s_{13}s_{23}e^{i\delta} & c_{12}c_{23} - s_{12}s_{13}s_{23}e^{i\delta} & c_{13}s_{23} \\ s_{12}s_{23} - c_{12}c_{23}s_{13}e^{i\delta} & -c_{23}s_{12}e^{i\delta}s_{13} - c_{12}s_{23} & c_{13}c_{23} \end{pmatrix}. \end{aligned} \tag{59}$$

This choice of active neutrino masses also satisfies the constraint from Plank2018 [114], $\sum_{i=a}^{3} m_{n_a} \leq 0.12$ eV.

The non-unitary part of the active neutrino mixing matrix $\left(I_3 - \frac{1}{2}RR^\dagger\right) U_{\rm PMNS}$ is constrained by other phenomenology such as EW precision [115–117], leading to a very strict constraint of $\eta \equiv \frac{1}{2}\left|RR^\dagger\right| \propto \hat{x}_\nu$ in the ISS framework [95,118,119]. The reasonable constraint of the non-unitary part of the neutrino mixing matrix is as follows:

$$x_0 \equiv \frac{m_{n_3}}{\mu_0} \leq 10^{-3}. \tag{60}$$

The other well-known numerical parameters are [102]:

$$g = 0.652,\ G_F = 1.1664 \times 10^{-5}\ \text{GeV},\ s_W^2 = 0.231,\ m_W = 80.385\ \text{GeV},$$
$$m_e = 5 \times 10^{-4}\ \text{GeV},\ m_\mu = 0.105\ \text{GeV},\ m_\tau = 1.776\ \text{GeV}. \tag{61}$$

For the free parameters of the 341ISS model, the numerical scanning ranges are:

$$M_0 \in [0.1,\ 10]\ \text{TeV},\ m_{h^\pm_{1,2}} \in [0.8,\ 10]\ \text{TeV},$$
$$t_\beta \in [0.3, 50],\ x_0 \in \left[10^{-6}, 10^{-3}\right],\ s_\alpha \in [-1, 1],\ |Y^d_{ab}| \leq 3.5,\ \forall a, b = 1, 2, 3. \tag{62}$$

In addition, we will fix $m_{n_1} = 0.01$ eV, and check the perturbative limit of all Yukawa couplings Y^σ and Y^ν, namely, $|Y^\sigma_{ab}|, |Y^\nu_{ab}| \leq 3.5$ must be satisfied. As we discussed above, the diagonal form of Y^d will allow large $(g-2)_{e_a}$ anomalies and small $\text{Br}(e_b \to e_a\gamma)$ satisfying the recent experimental constraints. In the numerical investigation, we will consider the general case that $Y^d_{ab} \neq 0$. The allowed regions of parameters we imply below must guarantee the experimental data of 1σ ranges of $(g-2)_{e,\mu}$, the cLFV constraints of $\text{Br}(e_b \to e_a\gamma)$, and the constraint of the decay $Z \to \mu^+\mu^-$ using the analytic formulas and experimental data given in Appendix B.

Now, we consider some particular different choices of zero entries of Y^d. The allowed regions of the parameter space predict some interesting properties. First, even with only Y^d_{11}, $Y^d_{22} \neq 0$, the allowed regions satisfying two $(g-2)_{e,\mu}$ data are still strictly constrained by the cLFV decay rate $\text{Br}(\mu \to e\gamma) < 4.2 \times 10^{-13}$, namely the constraints $|Y^d_{12}|, |Y^d_{21}| < 10^{-4}$ must be guaranteed. Therefore, we will fix $|Y^d_{12}| = |Y^d_{21}| = 0$ as the default values in our numerical investigations. Second, we give comments on the three following cases:

(1) $Y^d_{23} = Y^d_{32} = Y^d_{13} = Y^d_{31} = 0$, which is the case of Y^d being diagonal, as given in Eq. (56). The allowed regions of non-zero entries of Y^d are $0.02 \leq |Y^d_{11}| \leq 0.13$, $0.9 \leq |Y^d_{22}| \leq 2.5$, and $|Y^d_{33}| \leq 2.67$, see the left panel of Fig. 3. In this allowed region, $\text{Br}(\tau \to \mu\gamma)$ can reach the order of $\mathcal{O}(10^{-9})$, but predicts suppressed branching ratios $\text{Br}(\tau \to e\gamma) < 10^{-12}$, see the right panel of Fig. 3. We can see that $\text{Br}(\mu \to e\gamma)$ can reach the recent constraint of $\mathcal{O}(10^{-13})$ even when $Y^d_{12} = Y^d_{21} = 0$. This property is different from two other cLFV decays of τ, which are suppressed if $Y^d_{33} = 0$ is fixed, namely, $\text{Br}(\tau \to \mu\gamma) < 10^{-11}$. In addition, there exist regions that allow both small values of $\text{Br}(\mu \to e\gamma) \sim \mathcal{O}(10^{-14})$ corresponding to future experimental sensitivity and large $\Delta a_{e,\mu}$. In conclusion, we confirm that the formula of $a_{e,0}$ given in Eq. (54) is the main one-loop contribution to $(g-2)_{e_a}$ data and cLFV decay amplitudes. Hence, the diagonal form of Y^d results in small cLFV decay rates, even though they get contributions from other terms in Eq. (52).

(2) $Y^d_{32} = Y^d_{23} = Y^d_{33} = 0$ while Y^d_{31}, $Y^d_{31} \neq 0$. The two cLFV rates $\text{Br}(\tau \to e\gamma)$ and $\text{Br}(\mu \to e\gamma)$ can reach the recent experimental upper bound, while $\text{Br}(\tau \to \mu\gamma) < 3 \times 10^{-12}$. The allowed ranges of Y^d_{11} and Y^d_{22} are almost unchanged. The constraints of $Y^d_{13,31}$ are $|Y^d_{13}| < 0.67$ and $|Y^d_{31}| < 0.22$. Illustrations of relations between entries of Y^d and

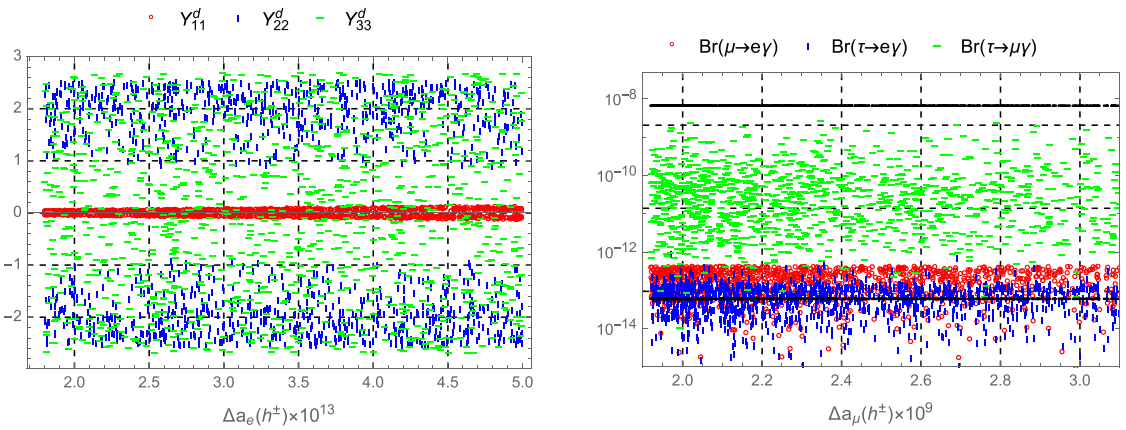

Fig. 3. The correlations between $\Delta a_\mu(h^\pm)$ vs Y^d_{aa} (left panel) and $\Delta a_e(h^\pm)$ vs Br($e_b \to e_a\gamma$) (right panel) in the case $Y^d_{23} = Y^d_{32} = Y^d_{13} = Y^d_{31} = 0$. The two black lines show the values of 6.9×10^{-9} and 6×10^{-14} corresponding to the future experimental sensitivities of cLFV decays $e_b \to e_a\gamma$ mentioned in the introduction.

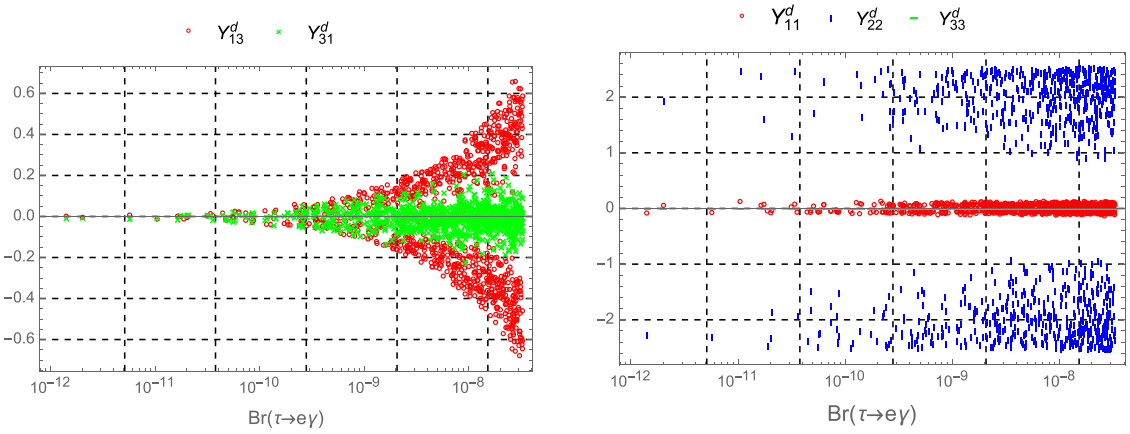

Fig. 4. The correlations between Br($\tau \to e\gamma$) vs $Y^d_{13,31}$ (left panel) and Y^d_{aa} (right panel) in the second case $Y^d_{23} = Y^d_{32} = Y^d_{33} = 0$.

Br($\tau \to e\gamma$) are presented in Fig. 4. We conclude that Br($\tau \to e\gamma$) depends strongly on Y^d_{13} and Y^d_{31}. In contrast, the allowed ranges of Y^d_{11} and Y^d_{22} mainly arise from the $(g-2)$ data.

(3) $Y^d_{13} = Y^d_{31} = Y^d_{33} = 0$ while Y^d_{32}, $Y^d_{2,3} \neq 0$. Two cLFV decays Br($\mu \to e\gamma$) and Br($\tau \to \mu\gamma$) can reach recent experimental bounds, but very suppressed Br($\tau \to e\gamma$) $< 10^{-12}$. The constraints of the non-zero entries of Y^d are $|Y^d_{23,32}| \leq 1$. Illustrations of Br($\tau \to \mu\gamma$) vs $Y^d_{23,32}$ and $a_{\mu,e}(h^\pm)$ are similar to case (2), hence we do not show them explicitly here.

We comment here on some properties of entries of Y^d derived from studying the three particular cases mentioned above. First, the diagonal entries of Y^d give main contributions to $(g-2)_{e_a}$ anomalies, whereas the non-zero entries $Y^d_{13,31}$ and $Y^d_{23,32}$ affect strongly the decay rates of Br($\tau \to e\gamma$) and Br($\tau \to \mu\gamma$), respectively. The Br($\mu \to e\gamma$) depends strongly on $Y^d_{12,21}$ and the combination of the remaining contributions. The recent experimental bound of Br($\mu \to e\gamma$) $< 4.2 \times 10^{-13}$ results in tiny values $|Y^d_{12,21}| < 10^{-4}$, hence we always fix these two entries as being

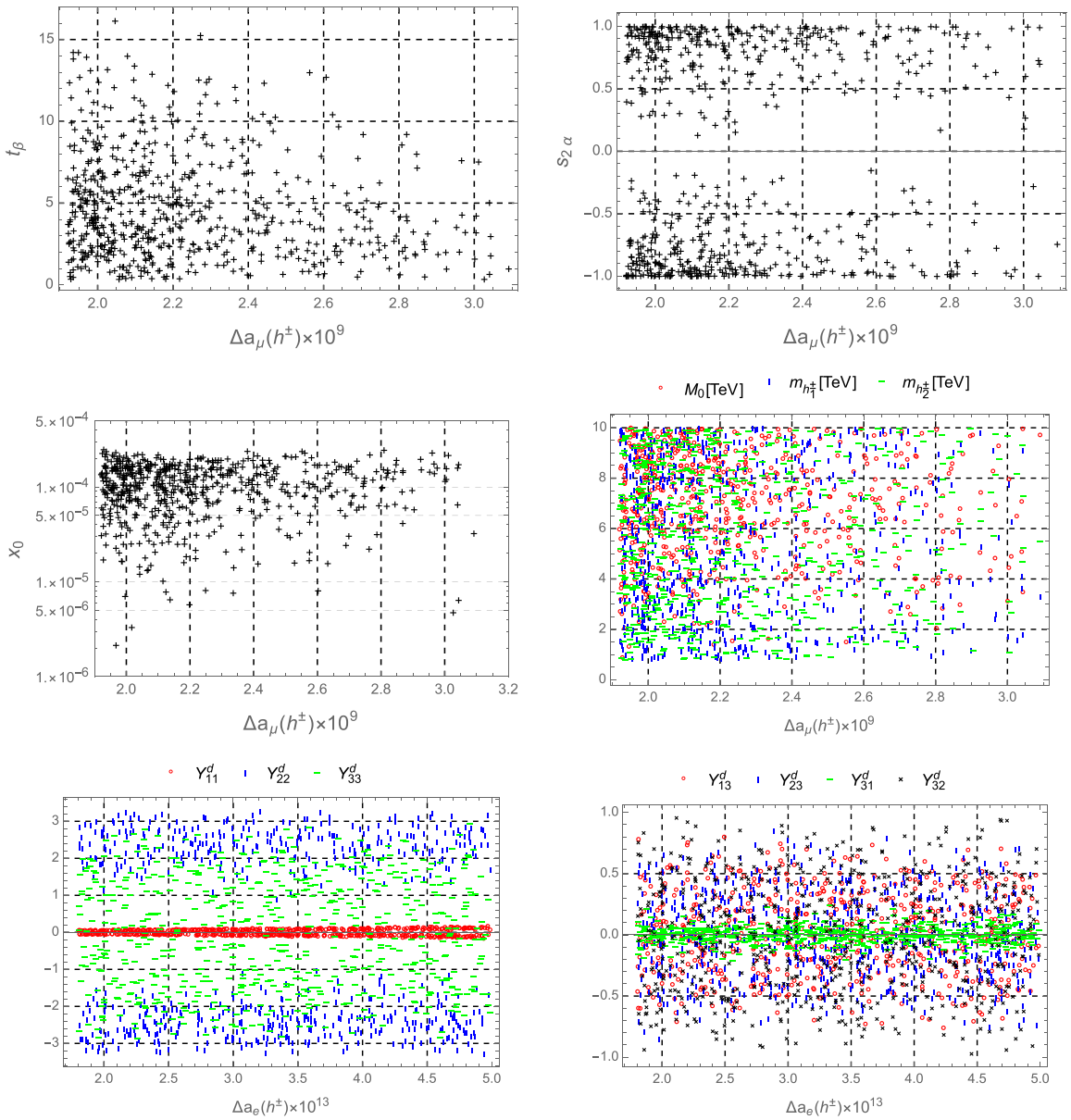

Fig. 5. The correlations between different free parameters vs $\Delta a_\mu(h^\pm)$ with $Y_{21} = Y_{12} = 0$.

zeros. We also emphasize that the negative sign of the experimental value of $\Delta a_e^{\rm NP}$ in Ref. [75] can be explained by the sign of Y_{22}^d.

In the final illustration, we consider the more general case that the only two zero entries of Y^d are $Y_{12}^d = Y_{21}^d = 0$. The correlations of important parameters vs $\Delta a_\mu(h^\pm)$ are shown in Fig. 5. The corresponding allowed ranges of the free parameters are:

$$
\begin{aligned}
&t_\beta \in [0.35, 16.14],\ s_\alpha \in [-0.988, -0.08] \cup [0.065, 0.996],\ x_0 \in \left[2.14 \times 10^{-6}, 2.5 \times 10^{-4}\right],\\
&M_0 \in [0.877, 10]\ [\text{TeV}],\ M_{1,2} \in [0.8, 10]\ [\text{TeV}],\\
&Y_{11}^d \in [-0.17, -0.03] \cup [0.022, 0.164],\ Y_{22}^d \in [-3.26, -1.03] \cup [0.909, 3.275],\ |Y_{33}^d| \le 2.93,\\
&Y_{13}^d \in [-0.76,\ 0.8],\ Y_{31}^d \in [-0.21,\ 0.25],\ Y_{23}^d \in [-0.85,\ 0.86],\ Y_{32}^d \in [-0.97,\ 0.96]. \qquad (63)
\end{aligned}
$$

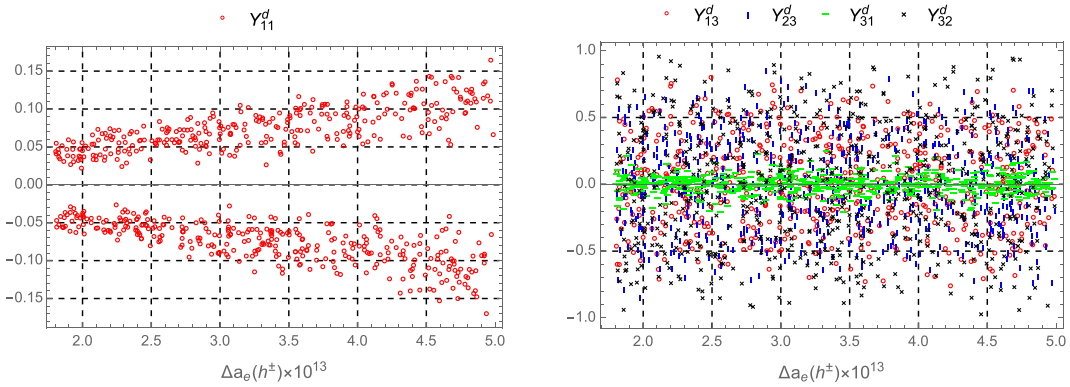

Fig. 6. The correlations between Y^d_{ij} vs $\Delta a_e(h^\pm)$ with $Y_{21} = Y_{12} = 0$.

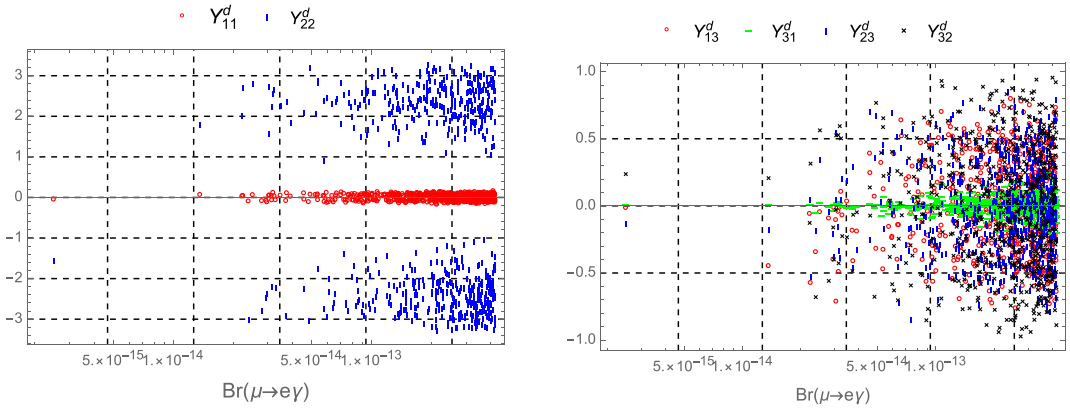

Fig. 7. The correlations between Y^d_{ij} vs $\text{Br}(\tau \to e\gamma, \mu\gamma)$ with $Y_{21} = Y_{12} = 0$.

We can see that many allowed ranges are stricter than the scanning ones given in Eq. (62). For example, large $(g-2)_{e,\,\mu}$ requires small t_β and large x_0 so that the new upper bound of t_β and lower bound of x_0 are determined. As a result, in Fig. 5, the allowed regions of small t_β and large x_0 are favored. Similarly, $a_{e_a,0} \propto s_\alpha c_\alpha = s_{2\alpha}/2$, therefore, the allowed values of large $s_{2\alpha}$ close to 1 are supported. In the bottom left panel, the allowed regions of $Y^d_{11,22}$ are the same as those predicted in Fig. 3, in which all non-diagonal entries are zeros. This implies that these regions are independent of non-diagonal entries of Y^d. Instead, large values of these entries favor the small $a_\mu(h^\pm)$, see the bottom right panel. As a result, small $(g-2)_\mu$ may predict large $\text{Br}(\tau \to \mu\gamma, \mu\gamma)$ and vice versa. In addition to explain both $(g-2)_{e_a}$ data of $\Delta a_\mu(h^\pm)$, the condition of $|m_{h^\pm_1} - m_{h^\pm_2}| \geq 523$ GeV is required, which is a condition derived from $a_{e_a,0}$ that $x_1 \neq x_2$. We emphasize that this model allows the existence of heavy charged Higgs bosons, which did not appear in some recent discussions on $(g-2)$ anomalies [24,25].

The relations of Y^d_{ij} vs $\Delta a_e(h^\pm)$ are shown in Fig. 6. In the left panel, $a_e(h^\pm) \propto |Y^d_{11}|$ confirms the relation given in Eq. (57). The $a_\mu(h^\pm) \propto |Y^d_{22}|$ is not very clear, because many points are excluded by the perturbative limit. The right panel shows that $a_e(h^\pm)$ does not give any prediction on Y^d_{ij} like the case of $a_\mu(h^\pm)$.

The correlations of Y^d_{ij} vs $\text{Br}(\mu \to e\gamma)$ are shown in Fig. 7. We see again that the constraints of Y^d_{ii} with $i = 1, 2$ are similar to those shown in the left panel of Fig. 3. This confirms the

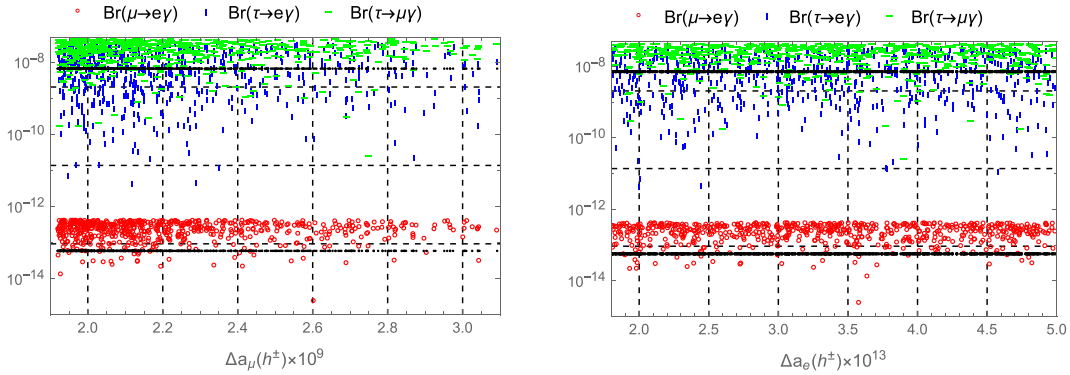

Fig. 8. The correlations between $\mathrm{Br}(e_b \to e_a\gamma)$ vs $\Delta a_{e,\,\mu}(h^\pm)$ with $Y_{21} = Y_{12} = 0$. The two black lines in each panel present the future experimental sensitivities of $\mathrm{Br}(e_b \to e_a\gamma)$ mentioned in the introduction.

conclusion that the allowed ranges of $Y^d_{11,22}$ are mainly controlled by the $(g-2)_{e_a}$ data. In the right panel of Fig. 7, large $\mathrm{Br}(\mu \to e\gamma)$ prefers large non-diagonal entries Y^d_{ij} but the small values are still allowed because of the destructive correlations between contributions from different parameters.

The correlations between $\Delta a_{e,\,\mu}$ and $\mathrm{Br}(e_b \to e_a\gamma)$ in the allowed regions of parameters listed in Eq. (63) are shown in Fig. 8. We can see that all allowed values of $a_{\mu,\,e}(h^\pm)$ in the 1σ experimental ranges still predict large $\mathrm{Br}(e_b \to e_a\gamma)$ near the current upper experimental bounds. Therefore, the future results of cLFV experiments, $(g-2)$ data, and neutrino oscillation will give stricter constraints on the allowed regions of the parameter space. Note also that future experimental constraints on other cLFV decays such as $\mu \to 3e < 10^{-16}$ [120] and $\mu - e$ conversion in nuclei [121] will be stricter than those considered in this work, but in general theoretical calculations on some other BSM in the presence of "chiral enhancement" show that they do not affect strongly the allowed regions we discussed above, see e.g. the left-right model [122]. From the theoretical side, this can be explained by the reason that the relevant one-loop corrections originated from one-loop four-point diagrams are proportional to the products of four vertex factors, therefore their numerical values are more flexible than the theoretical constraints from the cLFV decays $e_b \to e_a\gamma$. A more detailed investigation to predict the allowed regions corresponding to the future sensitivities of all interesting cLFV decays will be done in the future.

5. Conclusion

We have discussed a solution to explain the recent experimental data of the $(g-2)_{e_a}$ anomalies in the 341ISS framework. We have constructed the Yukawa Lagrangian of leptons and Higgs potential obeying the generalized lepton number $\mathcal{L}$ that keeps necessary terms generating the ISS mechanism and large chirally enhanced one-loop contributions to $(g-2)_{e_a}$ anomalies. Although the ISS mechanism may result in large cLFV decays $e_b \to e_a\gamma$, we have shown numerically that there always exist allowed regions of the parameter space guaranteeing these experimental bounds. In addition, these allowed regions will not be excluded totally if the future sensitivities of the cLFV experiments are updated, and no cLFV significations are found. The model can also explain successfully the existence of at least one of the cLFV decays $\tau \to \mu\gamma$, $e\gamma$, or $\mu \to e\gamma$ once they are detected by incoming experiments.

Acknowledgements
We thank Dr. Sumit Ghosh for useful discussions. We thank the referee for suggesting to us many interesting constraints. The future experimental sensitivities may result in important correlations of the model parameters, which will be investigated in more detail in our future work. This research is funded by Vietnam Ministry of Education and Training and Hanoi Pedagogical University 2 under grant number B.2021-SP2-05.

Appendix A. The SM-like Higgs boson

For simplicity in estimating the SM-like Higgs boson h found by the LHC, we assume some conditions of the Higgs self-couplings as follows:

$$\lambda_6 + \frac{fV}{2t_\beta w},\ \lambda_7 + \frac{fw}{2t_\beta V}, \lambda_8 + \frac{ft_\beta V}{2w}, \lambda_9 + \frac{fwt_\beta}{2V} \simeq 0. \tag{A1}$$

As a result, the SM-like Higgs boson gets dominant contributions from the neutral Higgs basis ($\mathrm{Re}[\rho_2^0]$, $\mathrm{Re}[\eta_1^0]$), corresponding to the following squared mass matrix:

$$\mathcal{M}_h^2 = \begin{pmatrix} 2\lambda_2 c_\beta^2 v^2 - \frac{ft_\beta V_w}{2} & \lambda_5 s_\beta c_\beta v^2 + \frac{fV_w}{2} \\ \lambda_5 s_\beta c_\beta v^2 + \frac{fV_w}{2} & 2\lambda_1 s_\beta^2 v^2 - \frac{fV_w}{2t_\beta} \end{pmatrix},$$

which results in one light CP-even neutral Higgs boson with mass

$$m_h^2 = 2\frac{\mathcal{M}_{h,11}^2\mathcal{M}_{h,22}^2 - \left(\mathcal{M}_{h,12}^2\right)^2}{\mathcal{M}_{h,11}^2 + \mathcal{M}_{h,22}^2 + \sqrt{\left(\mathcal{M}_{h,11}^2 - \mathcal{M}_{h,22}^2\right)^2 + 4\left(\mathcal{M}_{h,12}^2\right)^2}} \propto \mathcal{O}(v^2). \tag{A2}$$

Similarly, in the 2DHM framework, this CP-even Higgs boson can be identified with the SM-like Higgs boson found from the LHC. Denoting the mixing parameter α of these two Higgs bosons,

$$\begin{pmatrix} \mathrm{Re}[\rho_2^0] \\ \mathrm{Re}[\eta_1^0] \end{pmatrix} = \begin{pmatrix} c_\alpha & s_\alpha \\ -s_\alpha & c_\alpha \end{pmatrix} \begin{pmatrix} H \\ h \end{pmatrix}, \tag{A3}$$

the difference between the tree-level couplings $h\overline{e_a}e_a$ predicted by the model under consideration and the SM is a factor s_α/c_β, exactly the same as the 2HDM, see e.g. Ref. [123]. Therefore, the combination of this factor and the loop corrections can accommodate the experimental data.

Appendix B. One-loop corrections to $Z\mu^+\mu^-$ and $h\mu^+\mu^-$ vertices

The relations between the flavor and physical base of the neutral gauge bosons are [11]:

$$\begin{pmatrix} W_{3\mu} \\ W_{8\mu} \\ W_{15\mu} \\ B'_{4\mu} \end{pmatrix} = \begin{pmatrix} s_W & c_W & 0 & 0 \\ c_{32}c_W & -c_{32}s_W & -c_\theta s_{32} & s_{32}\,s_\theta \\ c_{43}c_W s_{32} & -c_{43}s_{32}s_W & c_{32}c_{43}\,c_\theta - s_{43}\,s_\theta & -c_\theta s_{43} - c_{32}c_{43}\,s_\theta \\ c_W s_{32}s_{43} & -s_{32}s_{43}s_W & c_{32}\,c_\theta s_{43} + c_{43}\,s_\theta & c_{43}\,c_\theta - c_{32}s_{43}\,s_\theta \end{pmatrix} \begin{pmatrix} A_\mu \\ Z_\mu \\ Z_{3\mu} \\ Z_{4\mu} \end{pmatrix}, \tag{B1}$$

where

$$s_{43} = \frac{\sqrt{3-6s_W^2}}{\sqrt{3-4s_W^2}},\ c_{43} = -\sqrt{1-c_{43}^2}, s_{32} = \frac{\sqrt{3-4s_W^2}}{c_W},\ c_{32} = \sqrt{1-c_{32}^2},$$
$$t_{2\theta} = \frac{s_{2\theta}}{c_{2\theta}} \sim \mathcal{O}(w^2/V^2). \tag{B2}$$

The matching relations from the breaking step $SU(4)_L \times U(1)_X \to SU(2)_L \times U(1)_Y$ are $W_3 = W_3$, $B_\mu = c_{32}W_{8\mu} + c_{43}s_{32}W_{15\mu} + s_{43}s_{32}B''_\mu$, and

$$\frac{1}{\sqrt{3}}T_8 - \frac{2}{\sqrt{6}}T_{15} + X\mathrm{I} = \frac{Y}{2}, \tag{B3}$$

where B_μ is the gauge boson of the gauge $U(1)_Y$ in the SM. The relation (B3) is consistent with the definition of the charge operator (4), the same as that given in the SM. This means that we can consider η and σ, ν_{aR} and X_{aR} as new scalars and neutral fermions giving one-loop corrections to the $Z\mu^+\mu^-$ couplings as discussed in Ref. [124]. Because all new neutral fermions are singlets, vertices $Z\nu_{aR}\bar{\nu}_{aR}$ and $ZX_{aR}\bar{X}_{aR}$ do not appear. Consequently, only diagram 2 of Fig. 1 in Ref. [124] is irrelevant to our model.

We use the result from Ref. [124] having the following Yukawa couplings that give one-loop correction to the $g^\mu_{L,R}$ of the vertex $Z\mu^+\mu^-$:

$$\mathcal{L}_Y = -y_L\bar{\mu}_L\phi_2\chi_R - y_R\bar{\mu}_R\phi\chi_L + \text{h.c.},$$

where s_k and $\chi_{L,R}$ are physical Higgs and fermion states, and $V_{k,l}$ is the Higgs mixing parameters relating to ϕ and ϕ_2 as follows: $\phi = V_{11}s_1 + V_{12}s_2$ and $\phi_2 = V_{21}s_1 + V_{22}s_2$. The vertex corrections are:

$$\begin{aligned}
\Delta g^\mu_L = \frac{y_L^2}{16\pi^2}\Bigg[& 2\sum_{k,l=1}^{2}\left\{\left(-\frac{1}{2} - Q_s s_W^2\right)V^*_{2k}V_{2l} - Q_s s_W^2 V^*_{1k}V_{1l}\right\}V_{2k}V^*_{2l}C_{24}(s_k, \chi, s_l; p, (q-p)) \\
& - \sum_{k=1}^{2}\left(-\frac{1}{2} + s_W^2\right)|V_{2k}|^2(B_0 + B_1)(s_k, \chi; p)\Bigg], \\
\Delta g^\mu_R = \frac{y_R^2}{16\pi^2}\Bigg[& 2\sum_{k,l=1}^{2}\left\{\left(-\frac{1}{2} - Q_s s_W^2\right)V^*_{2k}V_{2l} - Q_s s_W^2 V^*_{1k}V_{1l}\right\}V_{1k}V^*_{1l}C_{24}(s_k, \chi, s_l; p, (q-p)) \\
& - \sum_{k=1}^{2}s_W^2|V_{1k}|^2(B_0 + B_1)(s_k, \chi; p)\Bigg],
\end{aligned} \tag{B4}$$

where we have used $Q_\chi = 0$ for neutral fermions, and C_{24} and $B_{0,1}$ are Passarino–Veltman (PV) functions, which transform into the notations of LoopTools (LT) [125] as follows:

$$\begin{aligned}
&\{B_0, p^\mu B_1\}(A, B, p) \equiv 16\pi^2\mu^{2\epsilon}\int\frac{d^nk}{i(2\pi)^n}\frac{\{1,\ k^\mu\}}{\left[k^2 - m_A^2 + i\epsilon\right]\left[(k+p)^2 - m_B^2 + i\epsilon\right]} \\
&\quad = \{B_0, p^\mu B_1\}(p^2; m_A^2, m_B^2), \\
&\left\{p_1^\mu p_1^\nu C_{21} + p_2^\mu p_2^\nu C_{22} + (p_1^\mu p_2^\nu + p_2^\mu p_1^\nu)C_{23} + g^{\mu\nu}C_{24}\right\}(A, B, C; p_1, p_2) \\
&\quad = 16\pi^2\mu^{2\epsilon}\int\frac{d^nk}{i(2\pi)^n}\frac{\{1,\ k^\mu\}}{\left[k^2 - m_A^2 + i\epsilon\right]\left[(k+p_1)^2 - m_B^2 + i\epsilon\right] + \left[(k+p_1+p_2)^2 - m_C^2 + i\epsilon\right]} \\
&\quad = \left\{p_1^\mu p_1^\nu C_{11} + q^\mu q^\nu C_{22} + (p_1^\mu q^\nu + q^\mu p_1^\nu)C_{12} + g^{\mu\nu}C_{00}\right\}(p_1^2, p_2^2, q^2; m_A^2, m_B^2, m_C^2),
\end{aligned} \tag{B5}$$

where $B_{0,1}(p^2; m_A^2, m_B^2)$, and $C_{00,ij}(p_1^2, p_2^2, q^2; m_A^2, m_B^2, m_C^2)$ are LT notations, and $q = p_1 + p_2$. In the particular case of the decay $Z \to \mu^+\mu^-$, we apply the on-shell conditions that $q^2 = m_Z^2$ and $p_1^2 = p_2^2 = m_\mu^2 \simeq 0$.

The Yukawa part of Eq. (41) gives the following equivalence: $\eta_2^- = \phi_2$ and $\sigma^- \equiv \phi$ with $Q_\phi = Q_{\phi_2} = -1$, and new fermions are neutral singlets ν_{aR}, $X_{aR} \sim (1, 1, 0)$, which do not couple to

the Z boson. The mixing parameter of Higgs bosons in Eq. (28) gives

$$-s_\alpha = V_{11},\ c_\alpha = V_{12},\ V_{21} = c_\beta c_\alpha,\ V_{22} = c_\beta s_\alpha, \tag{B6}$$

and $h_k^- = s_k$. The Yukawa couplings in Eq. (42) in the basis of new physical neutral fermions read:

$$-\mathcal{L}_Y = \sum_{i=1}^{9}\sum_{a=1}^{3}\left[\frac{gM_0\left(\hat{x}_\nu^{1/2}U_{\rm PMNS}^{\nu*}\right)_{a2}}{\sqrt{2}m_W s_\beta}U_{(a+3)i}^{\nu*}\bar{L}_\mu \eta n_{iR} + Y_{a2}^{\sigma*}U_{(a+6)i}^{\nu}\overline{\mu_R}n_{iL}\sigma^-\right] + \text{h.c.}. \tag{B7}$$

For a new fermion $n_{iL,\,R}$ with $Q_{n_i} = 0$, we have

$$y_{iL} \equiv \sum_{a=1}^{3}\frac{gM_0\left(\hat{x}_\nu^{1/2}U_{\rm PMNS}^{\nu*}\right)_{a2}}{\sqrt{2}m_W s_\beta}U_{(a+3)i}^{\nu*},\ y_{iR} \equiv \sum_{a=1}^{3}Y_{a2}^{\sigma*}U_{(a+6)i}^{\nu},\ i = \overline{1,9}.$$

The vertex corrections to $Z\mu^+\mu^-$ in our work are:

$$\begin{aligned}
\Delta g_L^\mu &= \sum_{i=1}^{9}\frac{|y_{iL}|^2}{16\pi^2}\left[2\sum_{k,l=1}^{2}\left\{\left(-\frac{1}{2}+s_W^2\right)V_{2k}^*V_{2l} + s_W^2V_{1k}^*V_{1l}\right\}V_{2k}V_{2l}^*C_{00}\right.\\
&\quad\left. - \sum_{k=1}^{2}\left(-\frac{1}{2}+s_W^2\right)|V_{2k}|^2(B_0+B_1)\right]\\
&= \frac{g^2M_0^2}{32m_W^2s_\beta^2}\left[U_{\rm PMNS}^\dagger\hat{x}_\nu U_{\rm PMNS}\right]_{22}\left[2\sum_{k,l=1}^{2}\left\{\left(-\frac{1}{2}+s_W^2\right)V_{2k}^*V_{2l} + s_W^2V_{1k}^*V_{1l}\right\}V_{2k}V_{2l}^*C_{00}\right.\\
&\quad\left. - \sum_{k=1}^{2}\left(-\frac{1}{2}+s_W^2\right)|V_{2k}|^2(B_0+B_1)\right]\\
\Delta g_R^\mu &= \sum_{i=1}^{9}\frac{|y_{iR}|^2}{16\pi^2}\left[2\sum_{k,l=1}^{2}\left\{\left(-\frac{1}{2}+s_W^2\right)V_{2k}^*V_{2l} + s_W^2V_{1k}^*V_{1l}\right\}V_{1k}V_{1l}^*C_{00}\right.\\
&\quad\left. - \sum_{k=1}^{2}s_W^2|V_{1k}|^2(B_0+B_1)\right]\\
&= \frac{|Y^{\sigma\dagger}Y^\sigma|_{22}}{16\pi^2}\left[2\sum_{k,l=1}^{2}\left\{\left(-\frac{1}{2}+s_W^2\right)V_{2k}^*V_{2l} + s_W^2V_{1k}^*V_{1l}\right\}V_{1k}V_{1l}^*C_{00}\right.\\
&\quad\left. - \sum_{k=1}^{2}s_W^2|V_{1k}|^2(B_0+B_1)\right],
\end{aligned} \tag{B8}$$

where $C_{00} = C_{00}(0, 0, m_Z^2; m_{h_k^\pm}^2, M_0^2, m_{h_l^\pm}^2)$ and $B_{0,1} = B_{0,1}(0, m_{h_k}^2, M_0^2)$.

The following modified $Z\mu^+\mu^-$ couplings are

$$i\frac{g}{c_W}\gamma_\mu\left[\left(g_L^{\text{SM},\mu} + \Delta g_L^\mu\right)P_L + \left(g_R^{\text{SM},\mu} + \Delta g_R^\mu\right)P_R\right], \tag{B9}$$

where $g_L^{\text{SM},\mu} = -1/2 + s_W^2$, and $g_R^{\text{SM},\mu} = s_W^2$. Defining the following quantity [95]:

$$\delta R_{Ze_ae_a} \equiv \frac{\Gamma\left(Z\to e_a^+e_a^-\right)}{\Gamma_{\rm SM}\left(Z\to e_a^+e_a^-\right)} - 1 = \frac{|g_V|^2+|g_A|^2}{\left|g_V^{\rm SM}\right|^2+\left|g_Z^{\rm SM}\right|^2} - 1, \tag{B10}$$

where $g_{V,A}^{\rm SM} = g_R^{\rm SM} \pm g_L^{\rm SM}$, $g_V = g_V^{\rm SM} + \Delta g_L^\mu + \Delta g_R^\mu$, and $g_A = g_A^{\rm SM} - \Delta g_L^\mu + \Delta g_R^\mu$, the experimental constraint is: $-7 < \delta R_{Ze_ae_a}\times 10^3 < 6$ [95,102].

References

1 R. Foot, H. N. Long, and T. A. Tran, Phys. Rev. D **50**, R34 (1994) [arXiv:hep-ph/9402243] [Search inSPIRE].
2 F. Pisano and V. Pleitez, Phys. Rev. D **51**, 3865 (1995) [arXiv:hep-ph/9401272] [Search inSPIRE].
3 M. B. Voloshin, Sov. J. Nucl. Phys. **48**, 512 (1988), ITEP-87-215.
4 W. A. Ponce, D. A. Gutierrez, and L. A. Sanchez, Phys. Rev. D **69**, 055007 (2004) [arXiv:hep-ph/0312143] [Search inSPIRE].
5 L. A. Sanchez, F. A. Perez, and W. A. Ponce, Eur. Phys. J. C **35**, 259 (2004) [arXiv:hep-ph/0404005] [Search inSPIRE].
6 W. A. Ponce and L. A. Sanchez, Mod. Phys. Lett. A **22**, 435 (2007) [arXiv:hep-ph/0607175] [Search inSPIRE].
7 L. A. Sanchez, L. A. Wills-Toro, and J. I. Zuluaga, Phys. Rev. D **77**, 035008 (2008) [arXiv:0801.4044 [hep-ph]] [Search inSPIRE].
8 Riazuddin and Fayyazuddin, Eur. Phys. J. C **56**, 389 (2008) [arXiv:0803.4267 [hep-ph]] [Search inSPIRE].
9 S. H. Nam, K. Y. Lee, and Y. Y. Keum, Phys. Rev. D **82**, 105027 (2010) [arXiv:0909.3770 [hep-ph]] [Search inSPIRE].
10 G. Palacio, Int. J. Mod. Phys. A **31**, 1650142 (2016) [arXiv:1608.08676 [hep-ph]] [Search inSPIRE].
11 H. N. Long, L. T. Hue, and D. V. Loi, Phys. Rev. D **94**, 015007 (2016) [arXiv:1605.07835 [hep-ph]] [Search inSPIRE].
12 M. Djouala, N. Mebarki, and H. Aissaoui, Int. J. Mod. Phys. A **36**, 17 (2021) [arXiv:1911.04887 [hep-ph]] [Search inSPIRE].
13 D. Cogollo, Y. M. Oviedo-Torres, and Y. S. Villamizar, Int. J. Mod. Phys. A **35**, 2050126 (2020) [arXiv:2004.14792 [hep-ph]] [Search inSPIRE].
14 L. T. Hue, K. H. Phan, T. P. Nguyen, H. N. Long, and H. T. Hung, Eur. Phys. J. C **82**, 722 (2022) [arXiv:2109.06089 [hep-ph]] [Search inSPIRE].
15 A. Palcu, Mod. Phys. Lett. A **24**, 2589 (2009) [arXiv:0908.1636 [hep-ph]] [Search inSPIRE].
16 A. Palcu, Int. J. Theor. Phys. **56**, 403 (2017) [arXiv:1510.06717 [hep-ph]] [Search inSPIRE].
17 J. P. Pinheiro, C. A. de S. Pires, F. S. Queiroz, and Y. S. Villamizar, Phys. Lett. B **823**, 136764 (2021) [arXiv:2107.01315 [hep-ph]] [Search inSPIRE].
18 K. Y. Lee and S. H. Nam, J. Phys. G **42**, 125003 (2015) [arXiv:1412.1541 [hep-ph]] [Search inSPIRE].
19 A. Crivellin, M. Hoferichter, and P. Schmidt-Wellenburg, Phys. Rev. D **98**, 113002 (2018) [arXiv:1807.11484 [hep-ph]] [Search inSPIRE].
20 X. F. Han, T. Li, L. Wang, and Y. Zhang, Phys. Rev. D **99**, 095034 (2019) [arXiv:1812.02449 [hep-ph]] [Search inSPIRE].
21 M. Endo and W. Yin, JHEP **08**, 122 (2019) [arXiv:1906.08768 [hep-ph]] [Search inSPIRE].
22 M. Abdullah, B. Dutta, S. Ghosh, and T. Li, Phys. Rev. D **100**, 115006 (2019) [arXiv:1907.08109 [hep-ph]] [Search inSPIRE].
23 E. J. Chun and T. Mondal, JHEP **11**, 077 (2020) [arXiv:2009.08314 [hep-ph]] [Search inSPIRE].
24 L. Delle Rose, S. Khalil, and S. Moretti, Phys. Lett. B **816**, 136216 (2021) [arXiv:2012.06911 [hep-ph]] [Search inSPIRE].
25 F. J. Botella, F. Cornet-Gomez, and M. Nebot, Phys. Rev. D **102**, 035023 (2020) [arXiv:2006.01934 [hep-ph]] [Search inSPIRE].
26 S. P. Li, X. Q. Li, Y. Y. Li, Y. D. Yang, and X. Zhang, JHEP **01**, 034 (2021) [arXiv:2010.02799 [hep-ph]] [Search inSPIRE].
27 I. Bigaran and R. R. Volkas, Phys. Rev. D **102**, 075037 (2020) [arXiv:2002.12544 [hep-ph]] [Search inSPIRE].
28 X. F. Han, T. Li, H. X. Wang, L. Wang, and Y. Zhang, Phys. Rev. D **104**, 115001 (2021) [arXiv:2104.03227 [hep-ph]] [Search inSPIRE].
29 H. Bharadwaj, S. Dutta, and A. Goyal, JHEP **11**, 056 (2021) [arXiv:2109.02586 [hep-ph]] [Search inSPIRE].
30 C. Arbeláez, R. Cepedello, R. M. Fonseca, and M. Hirsch, Phys. Rev. D **102**, 075005 (2020) [arXiv:2007.11007 [hep-ph]] [Search inSPIRE].

31 K. F. Chen, C. W. Chiang, and K. Yagyu, JHEP **09**, 119 (2020) [arXiv:2006.07929 [hep-ph]] [Search inSPIRE].
32 B. Dutta, S. Ghosh, and T. Li, Phys. Rev. D **102**, 055017 (2020) [arXiv:2006.01319 [hep-ph]] [Search inSPIRE].
33 A. E. C. Hernández, S. F. King, and H. Lee, Phys. Rev. D **103**, 115024 (2021) [arXiv:2101.05819 [hep-ph]] [Search inSPIRE].
34 A. E. C. Hernández, D. T. Huong, and I. Schmidt, Eur. Phys. J. C **82**, 63 (2022) [arXiv:2109.12118 [hep-ph]] [Search inSPIRE].
35 S. Li, Z. Li, F. Wang, and J. M. Yang, Nucl. Phys. B **983**, 115927 (2022) [arXiv:2205.15153 [hep-ph]] [Search inSPIRE].
36 F. J. Botella, F. Cornet-Gomez, C. Miró, and M. Nebot, Eur. Phys. J. C **82**, 915 (2022) [arXiv:2205.01115 [hep-ph]] [Search inSPIRE].
37 L. Wang, J. M. Yang, and Y. Zhang, Commun. Theor. Phys. **74**, 097202 (2022) [arXiv:2203.07244 [hep-ph]] [Search inSPIRE].
38 J. Kriewald, J. Orloff, E. Pinsard, and A. M. Teixeira, Eur. Phys. J. C **82**, 844 (2022) [arXiv:2204.13134 [hep-ph]] [Search inSPIRE].
39 R. K. Barman, R. Dcruz, and A. Thapa, JHEP **03**, 183 (2022) [arXiv:2112.04523 [hep-ph]] [Search inSPIRE].
40 R. Dermisek, Moscow Univ. Phys. Bull. **77**, 102 (2022) [arXiv:2201.06179 [hep-ph]] [Search inSPIRE].
41 T. A. Chowdhury, M. Ehsanuzzaman, and S. Saad, JCAP **08**, 076 (2022) [arXiv:2203.14983 [hep-ph]] [Search inSPIRE].
42 C. H. Chen, C. W. Chiang, and C. W. Su, "Top-quark FCNC decays, LFVs, lepton $g-2$, and W mass anomaly with inert charged Higgses,"[arXiv:2301.07070 [hep-ph]] [Search inSPIRE].
43 B. Abi et al. [Muon g-2], Phys. Rev. Lett. **126**, 141801 (2021) [arXiv:2104.03281 [hep-ex]] [Search inSPIRE].
44 G. W. Bennett et al. [Muon g-2], Phys. Rev. D **73**, 072003 (2006) [arXiv:hep-ex/0602035 [hep-ex]] [Search inSPIRE].
45 T. Aoyama et al. Phys. Rept. **887**, 1 (2020) [arXiv:2006.04822 [hep-ph]] [Search inSPIRE].
46 M. Davier, A. Hoecker, B. Malaescu, and Z. Zhang, Eur. Phys. J. C **71**, 1515 (2011); **72**, 1874 (2012) [erratum][arXiv:1010.4180 [hep-ph]] [Search inSPIRE].
47 T. Aoyama, M. Hayakawa, T. Kinoshita, and M. Nio, Phys. Rev. Lett. **109**, 111808 (2012) [arXiv:1205.5370 [hep-ph]] [Search inSPIRE].
48 T. Aoyama, T. Kinoshita, and M. Nio, Atoms **7**, 28 (2019).
49 A. Czarnecki, W. J. Marciano, and A. Vainshtein, Phys. Rev. D **67**, 073006 (2003); **73**, 119901 (2006) [erratum][arXiv:hep-ph/0212229] [Search inSPIRE].
50 C. Gnendiger, D. Stöckinger, and H. Stöckinger-Kim, Phys. Rev. D **88**, 053005 (2013) [arXiv:1306.5546 [hep-ph]] [Search inSPIRE].
51 I. Danilkin and M. Vanderhaeghen, Phys. Rev. D **95**, 014019 (2017) [arXiv:1611.04646 [hep-ph]] [Search inSPIRE].
52 M. Davier, A. Hoecker, B. Malaescu, and Z. Zhang, Eur. Phys. J. C **77**, 827 (2017) [arXiv:1706.09436 [hep-ph]] [Search inSPIRE].
53 A. Keshavarzi, D. Nomura, and T. Teubner, Phys. Rev. D **97**, 114025 (2018) [arXiv:1802.02995 [hep-ph]] [Search inSPIRE].
54 G. Colangelo, M. Hoferichter, and P. Stoffer, JHEP **02**, 006 (2019) [arXiv:1810.00007 [hep-ph]] [Search inSPIRE].
55 M. Hoferichter, B. L. Hoid, and B. Kubis, JHEP **08**, 137 (2019) [arXiv:1907.01556 [hep-ph]] [Search inSPIRE].
56 M. Davier, A. Hoecker, B. Malaescu, and Z. Zhang, Eur. Phys. J. C **80**, 241 (2020); **80**, 410 (2020) [erratum] [arXiv:1908.00921 [hep-ph]][Search inSPIRE].
57 A. Keshavarzi, D. Nomura, and T. Teubner, Phys. Rev. D **101**, 014029 (2020) [arXiv:1911.00367 [hep-ph]] [Search inSPIRE].
58 A. Kurz, T. Liu, P. Marquard, and M. Steinhauser, Phys. Lett. B **734**, 144 (2014) [arXiv:1403.6400 [hep-ph]] [Search inSPIRE].
59 K. Melnikov and A. Vainshtein, Phys. Rev. D **70**, 113006 (2004) [arXiv:hep-ph/0312226] [Search inSPIRE].

60 P. Masjuan and P. Sanchez-Puertas, Phys. Rev. D **95**, 054026 (2017) [arXiv:1701.05829 [hep-ph]] [Search inSPIRE].
61 G. Colangelo, M. Hoferichter, M. Procura, and P. Stoffer, JHEP **04**, 161 (2017) [arXiv:1702.07347 [hep-ph]] [Search inSPIRE].
62 M. Hoferichter, B. L. Hoid, B. Kubis, S. Leupold, and S. P. Schneider, JHEP **10**, 141 (2018) [arXiv:1808.04823 [hep-ph]] [Search inSPIRE].
63 A. Gérardin, H. B. Meyer, and A. Nyffeler, Phys. Rev. D **100**, 034520 (2019) [arXiv:1903.09471 [hep-lat]] [Search inSPIRE].
64 J. Bijnens, N. Hermansson-Truedsson, and A. Rodríguez-Sánchez, Phys. Lett. B **798**, 134994 (2019) [arXiv:1908.03331 [hep-ph]] [Search inSPIRE].
65 G. Colangelo, F. Hagelstein, M. Hoferichter, L. Laub, and P. Stoffer, JHEP **03**, 101 (2020) [arXiv:1910.13432 [hep-ph]] [Search inSPIRE].
66 T. Blum, N. Christ, M. Hayakawa, T. Izubuchi, L. Jin, C. Jung, and C. Lehner, Phys. Rev. Lett. **124**, 132002 (2020) [arXiv:1911.08123 [hep-lat]] [Search inSPIRE].
67 G. Colangelo, M. Hoferichter, A. Nyffeler, M. Passera, and P. Stoffer, Phys. Lett. B **735**, 90–91 (2014) [arXiv:1403.7512 [hep-ph]] [Search inSPIRE].
68 V. Pauk and M. Vanderhaeghen, Eur. Phys. J. C **74**, 3008 (2014) [arXiv:1401.0832 [hep-ph]] [Search inSPIRE].
69 F. Jegerlehner, Springer Tracts Mod. Phys. **274**, 1 (2017).
70 M. Knecht, S. Narison, A. Rabemananjara, and D. Rabetiarivony, Phys. Lett. B **787**, 111 (2018) [arXiv:1808.03848 [hep-ph]] [Search inSPIRE].
71 G. Eichmann, C. S. Fischer, and R. Williams, Phys. Rev. D **101**, 054015 (2020) [arXiv:1910.06795 [hep-ph]] [Search inSPIRE].
72 P. Roig and P. Sanchez-Puertas, Phys. Rev. D **101**, 074019 (2020) [arXiv:1910.02881 [hep-ph]] [Search inSPIRE].
73 S. Borsanyi et al. Nat. **593**, 51 (2021) [arXiv:2002.12347 [hep-lat]] [Search INSPIRE].
74 D. Hanneke, S. Fogwell, and G. Gabrielse, Phys. Rev. Lett. **100**, 120801 (2008) [arXiv:0801.1134 [physics.atom-ph]] [Search inSPIRE].
75 R. H. Parker, C. Yu, W. Zhong, B. Estey, and H. Müller, Sci. **360**, 191 (2018) [arXiv:1812.04130 [physics.atom-ph]] [Search inSPIRE].
76 L. Morel, Z. Yao, P. Cladé, and S. Guellati-Khélifa, Nat. **588**, 61 (2020).
77 X. Fan, T. G. Myers, B. A. D. Sukra, and G. Gabrielse, Phys. Rev. Lett. **130**, 071801 (2023) [arXiv:2209.13084 [physics.atom-ph]] [Search inSPIRE].
78 T. Aoyama, M. Hayakawa, T. Kinoshita, and M. Nio, Phys. Rev. Lett. **109**, 111807 (2012) [arXiv:1205.5368 [hep-ph]] [Search inSPIRE].
79 S. Laporta, Phys. Lett. B **772**, 232 (2017) [arXiv:1704.06996 [hep-ph]] [Search inSPIRE].
80 T. Aoyama, T. Kinoshita, and M. Nio, Phys. Rev. D **97**, 036001 (2018) [arXiv:1712.06060 [hep-ph]] [Search inSPIRE].
81 H. Terazawa, Nonlin. Phenom. Complex Syst. **21**, 268 (2018).
82 S. Volkov, Phys. Rev. D **100**, 096004 (2019) [arXiv:1909.08015 [hep-ph]] [Search inSPIRE].
83 A. Gérardin, Eur. Phys. J. A **57**, 116 (2021) [arXiv:2012.03931 [hep-lat]] [Search inSPIRE].
84 B. Aubert et al. [BaBar], Phys. Rev. Lett. **104**, 021802 (2010) [arXiv:0908.2381 [hep-ex]] [Search inSPIRE].
85 A. M. Baldini et al. [MEG], Eur. Phys. J. C **76**, 434 (2016) [arXiv:1605.05081 [hep-ex]] [Search inSPIRE].
86 A. Abdesselam et al. [Belle], JHEP **10**, 19 (2021) [arXiv:2103.12994 [hep-ex]] [Search inSPIRE].
87 A. M. Baldini et al. [MEG II], Eur. Phys. J. C **78**, 380 (2018) [arXiv:1801.04688 [physics.ins-det]] [Search inSPIRE].
88 E. Kou et al. [Belle-II], Prog. Theor. Exp. Phys. **2019**, 123C01 (2019); **2020**, 029201 (2020) [erratum][arXiv:1808.10567 [hep-ex]] [Search inSPIRE].
89 S. Banerjee et al., "Snowmass 2021 White Paper: Charged lepton flavor violation in the tau sector,"[arXiv:2203.14919 [hep-ph]] [Search inSPIRE].
90 A. E. Cárcamo Hernández, L. Duarte, A. S. de Jesus, S. Kovalenko, F. S. Queiroz, C. Siqueira, Y. M. Oviedo-Torres, and Y. Villamizar, Phys. Rev. D **107**, 063005 (2023) [arXiv:2208.08462 [hep-ph]] [Search inSPIRE].
91 V. Oliveira and C. A. D. S. Pires, [arXiv:2208.00420 [hep-ph]] [Search inSPIRE].

92 H. Georgi, Lie Algebras in Particle Physics: From Isospin to Unified Theories (Taylor & Francis, Boca Raton, FL, 2000).
93 D. Chang and H. N. Long, Phys. Rev. D **73**, 053006 (2006) [arXiv:hep-ph/0603098] [Search inSPIRE].
94 L. T. Hue, A. E. Cárcamo Hernández, H. N. Long, and T. T. Hong, Nucl. Phys. B **984**, 115962 (2022) [arXiv:2110.01356 [hep-ph]] [Search inSPIRE].
95 P. Escribano, J. Terol-Calvo, and A. Vicente, Phys. Rev. D **103**, 115018 (2021) [arXiv:2104.03705 [hep-ph]] [Search inSPIRE].
96 A. Crivellin and M. Hoferichter, "The Anomalous Magnetic Moment of the Muon: Beyond the Standard Model via Chiral Enhancement," [arXiv:2207.01912 [hep-ph]] [Search inSPIRE].
97 A. Crivellin and M. Hoferichter, JHEP **07**, 135 (2021); **10**, 030 (2022) [erratum][arXiv:2104.03202 [hep-ph]] [Search inSPIRE].
98 R. Dermisek and A. Raval, Phys. Rev. D **88**, 013017 (2013) [arXiv:1305.3522 [hep-ph]] [Search in SPIRE].
99 A. M. Sirunyan et al. [CMS], JHEP **01**, 148 (2021) [arXiv:2009.04363 [hep-ex]] [Search inSPIRE].
100 G. Aad et al. [ATLAS], Phys. Lett. B **812**, 135980 (2021) [arXiv:2007.07830 [hep-ex]] [Search inSPIRE].
101 F. Jegerlehner and A. Nyffeler, Phys. Rept. **477**, 1 (2009) [arXiv:0902.3360 [hep-ph]] [Search inSPIRE].
102 P. A. Zyla et al. [Particle Data Group], Prog. Theor. Exp. Phys. **2020**, 083C01 (2020).
103 J. A. Casas and A. Ibarra, Nucl. Phys. B **618**, 171 (2001) [arXiv:hep-ph/0103065] [Search inSPIRE].
104 B. Pontecorvo, Sov. Phys. JETP **6**, 429 (1957).
105 Z. Maki, M. Nakagawa, and S. Sakata, Prog. Theor. Phys. **28**, 870 (1962).
106 E. Arganda, M. J. Herrero, X. Marcano, and C. Weiland, Phys. Rev. D **91**, 015001 (2015). [arXiv:1405.4300 [hep-ph]] [Search inSPIRE].
107 N. H. Thao, L. T. Hue, H. T. Hung, and N. T. Xuan, Nucl. Phys. B **921**, 159 (2017) [arXiv:1703.00896 [hep-ph]] [Search inSPIRE].
108 L. Lavoura, Eur. Phys. J. C **29**, 191 (2003) [arXiv:hep-ph/0302221] [Search inSPIRE].
109 L. T. Hue, L. D. Ninh, T. T. Thuc, and N. T. T. Dat, Eur. Phys. J. C **78**, 128 (2018) [arXiv:1708.09723 [hep-ph]] [Search inSPIRE].
110 G. W. Bennett et al. [Muon (g-2)], Phys. Rev. D **80**, 052008 (2009) [arXiv:0811.1207 [hep-ex]] [Search inSPIRE].
111 T. S. Roussy et al., "A new bound on the electron's electric dipole moment,"[arXiv:2212.11841 [physics.atom-ph]] [Search inSPIRE].
112 L. T. Hue, H. T. Hung, N. T. Tham, H. N. Long, and T. P. Nguyen, Phys. Rev. D **104**, 033007 (2021) [arXiv:2104.01840 [hep-ph]] [Search inSPIRE].
113 T. T. Hong, N. H. T. Nha, T. P. Nguyen, L. T. T. Phuong, and L. T. Hue, Prog. Theor. Exp. Phys. **2022**, 093B05 (2022) [arXiv:2206.08028 [hep-ph]] [Search inSPIRE].
114 N. Aghanim et al. [Planck], Astron. Astrophys. **641**, A6 (2020); **652**, C4 (2021) [erratum][arXiv:1807.06209 [astro-ph.CO]] [Search inSPIRE].
115 E. Fernandez-Martinez, J. Hernandez-Garcia, and J. Lopez-Pavon, JHEP **08**, 033 (2016) [arXiv:1605.08774 [hep-ph]] [Search inSPIRE].
116 N. R. Agostinho, G. C. Branco, P. M. F. Pereira, M. N. Rebelo, and J. I. Silva-Marcos, Eur. Phys. J. C **78**, 895 (2018) [arXiv:1711.06229 [hep-ph]] [Search inSPIRE].
117 A. M. Coutinho, A. Crivellin, and C. A. Manzari, Phys. Rev. Lett. **125**, 071802 (2020) [arXiv:1912.08823 [hep-ph]] [Search inSPIRE].
118 C. Biggio, E. Fernandez-Martinez, M. Filaci, J. Hernandez-Garcia, and J. Lopez-Pavon, JHEP **05**, 022 (2020) [arXiv:1911.11790 [hep-ph]] [Search inSPIRE].
119 T. Mondal and H. Okada, Nucl. Phys. B **976**, 115716 (2022) [arXiv:2103.13149 [hep-ph]] [Search inSPIRE].
120 A. Blondel, et al., "Research Proposal for an Experiment to Search for the Decay $\mu \to eee$,"[arXiv:1301.6113 [physics.ins-det]] [Search inSPIRE].
121 F. Abdi et al. [Mu2e], Universe **9**, 54 (2023) [arXiv:2210.11380 [hep-ex]] [Search inSPIRE].
122 M. Ashry, K. Ezzat, and S. Khalil, Phys. Rev. D **107**, 055044 (2023) [arXiv:2207.05828 [hep-ph]] [Search inSPIRE].

123 T. P. Nguyen, T. T. Thuc, D. T. Si, T. T. Hong, and L. T. Hue, Prog. Theor. Exp. Phys. **2022**, 023B01 (2022) [arXiv:2011.12181 [hep-ph]] [Search INSPIRE].
124 S. Kanemitsu and K. Tobe, Phys. Rev. D **86**, 095025 (2012) [arXiv:1207.1313 [hep-ph]] [Search in SPIRE].
125 T. Hahn and M. Perez-Victoria, Comput. Phys. Commun. **118**, 153 (1999) [arXiv:hep-ph/9807565] [Search inSPIRE].